Measurements of Nearshore Waves through Coherent Arrays of Small-Scale, Free-Drifting Wave Buoys

Edwin John Rainville

A thesis
submitted in partial fulfillment of the
requirements for the degree of

Master of Science

University of Washington

2022

Committee:

Jim Thomson, Chair

Melissa Moulton, Chair

Morteza Derakhti, Chair

Program Authorized to Offer Degree:
Civil and Environmental Engineering

University of Washington

Abstract

Measurements of Nearshore Waves through Coherent Arrays of Small-Scale, Free-Drifting Wave Buoys

Edwin John Rainville

Co-Chairs of the Supervisory Committee:
Jim Thomson
Department of Civil & Environmental Engineering

Melissa Moulton
Department of Civil & Environmental Engineering

Morteza Derakhti
Department of Civil & Environmental Engineering

Along the coastlines, surface gravity wave breaking occurs in complex spatial and temporal patterns that have significant impacts on coastal erosion, transport of scalars and coastal flooding. Numerical models are used to predict these processes but many models lack validation against measurements during storm events. To fill the need for more nearshore wave measurements during extreme conditions, we created a large dataset of measurements of nearshore waves through the deployment of coherent arrays of small-scale, free-drifting wave buoys called microSWIFTs. The measurements were collected over a 27-day field experiment in October of 2021 at the US Army Corps of Engineers Field Research Facility in Duck, NC. The microSWIFT wave buoy developed in this project is a scaled-down cylindrical version of the original SWIFT (Surface Wave Instrumentation Float with Tracking) wave buoy with a length of 21 cm and a diameter of 9 cm. The microSWIFT is equipped with a GPS module and Inertial Measurement Unit (IMU), where the global position, horizontal velocities, rotation rates, accelerations, and heading of the buoy are all measured directly and vertical velocity and sea surface elevation are computed from these measurements. While many

other small wave buoys have been developed, the deployment of the microSWIFTs as large coherent arrays is a novel deployment strategy for surf zone drifters and leads to more robust statistics of measurements and the ability to observe larger spatial areas. The dataset spans 1,154 individual microSWIFT drifts over a range of 73 separate coherent arrays. Over all of the separate coherent arrays, 24.7 hours of data were recorded during the experiment. The offshore wave conditions during the field experiment had significant wave heights ranging from 0.1 meters to 3 meters and peak wave periods ranging from 4 seconds to 20 seconds over the entire experiment. This dataset is used to investigate the transformation of waves in the surf zone and the location of individual breaking waves. Future goals using this dataset are to test and validate phase-resolved and phase-averaged wave models in the nearshore environment.

TABLE OF CONTENTS

LIST OF FIGURES

LIST OF TABLES

ACKNOWLEDGMENTS

I would first like to thank Jim Thomson, Melissa Moulton and Morteza Derakhti for your guidance, excitement, patience and caring over these past couple of years. It has been a blast and I am looking forward to continuing working with you all in the future. I would also like to thank my wonderful parents, sister and friends that have supported me along the way, this process has been far more enjoyable with them and could not have been done without them. Also a special thank you to Anna McDonald for the continuous listening, support and fun discussions along the way, you may be able to present this work even better than I can at this point.

This project would still be in our minds if it weren't for the excellent engineering work of Alex de Klerk, Joe Talbert, Nate Clemmet and Emily Iseley and their design and manufacturing work on the microSWIFT buoys, as well as support in the field experiment. Support from the Environmental Fluid Mechanics group and in particular the students Emma Nuss, Christine Baker and Jake Davis for helping with the field work on this project, humoring my questions and generally being fantastic peers.

I also would like to thank the faculty and staff members from the US Army Corps of Engineers Field Research Facility for all the support in operations and always offering a helping hand when we needed it. Along with the help from the Town of Duck surf rescue members for deploying some of the microSWIFTs and helping with recovering the buoys when they went too far offshore. These data were collected as part of the During Nearshore Event Experiment (DUNEX), which was facilitated by the U.S. Coastal Research Program (USCRP). We thank USCRP for their support of this effort through funding for logistics and coordination.

Chapter 1

INTRODUCTION AND MOTIVATION

The oceans cover the majority of the surface of the earth (approximately 70%) and about 60% of the people on earth live near the coasts [*Boehm et al.*, 2017; *Vitousek et al.*, 1997]. The coastlines of the world are complex, interesting, and important environments to both care for and be wary of. Due to climate change, sea levels are rising and storm frequency and intensity is increasing thus making the coastlines more susceptible to coastal flooding, infrastructure damage, and loss of life [*Michener et al.*, 1997]. During storms, increases in mean sea level height due to atmospheric pressure gradients and coastal sea state are known as storm surges [*Bertin*, 2016]. The increase in mean sea level can result in flooding which can be very damaging to coastal communities and ecosystems [*Bertin*, 2016]. Hurricane Sandy, which impacted the east coast of the US in 2012, led to an estimated $50 billion in direct and indirect costs *Abel et al.* [2012]. Under moderate green house gas emission forcing scenarios, $990 billion in damages to the coastlines is predicted between now and the year 2100 due to storm surge and sea level rise [*Neumann et al.*, 2015]. While the wind is the largest contributor to storm surges, the waves generated by the wind can amplify storm surge by tens of centimeters, which for low-lying areas can be detrimental [*Bertin*, 2016]. To appropriately manage the coastlines, we use operational wave models to forecast the conditions and then act accordingly. However, most operational wave models tend to underestimate the peaks of extreme storm events [*Cavaleri*, 2009]. To best protect ourselves and appropriately manage the coastal oceans we must improve our understanding of the coastal ocean system through measurements of the coastal ocean in many different conditions ranging from ambient to extreme.

1.0.1 Overview of Nearshore Processes

The coastal oceans can be are split into many different regions. These regions are dynamically distinct and examples are shown for a typical beach in Figure 1.1 originally from [*Jackson and Short*, 2020]. The swash zone is the first region from the beach heading offshore followed by the inner surf zone. Following the inner surf zone is the outer surf zone which is characterized by the region of the coastal ocean where depth-limited wave breaking is the main driver of the hydrodynamics [*Battjes*, 1988]. Past the surf zone is the shoaling zone where waves steepen in shallow water. The shoaling zone is then followed by the inner shelf which extends from the edge of the surf zone to approximately 1.5 km offshore [*Lentz and Fewings*, 2012].

In the inner shelf and surf zone, the wind and wave forcing is balanced by the bottom stress [*Feddersen et al.*, 1998]. In the inner shelf, the wind contributes approximately one-third of the forcing while the wave forcing makes up the majority of the forcing [*Feddersen et al.*, 1998]. However, within the surf zone, the effects of wind are mostly unimportant while outside the surf zone the effects of wind are very important to the momentum budget [*Feddersen et al.*, 1998]. In the inner shelf, the vertical structure of dissipation is characterized by a maximum at the surface, a minimum at mid-depth and another smaller maximum near the bottom. This vertical structure does not agree with turbulence scaling within the surf zone [*Feddersen et al.*, 2007]. Inside the surf zone, surface generated turbulence from breaking waves is the dominant source of turbulence while the bottom generated turbulence is small but still important [*Grasso and Ruessink*, 2011]. The turbulence generated by individual breaking waves can stir the water and suspend sediment which leads to beach erosion and geomorphology changes [*Butt et al.*, 2004].

The water circulation in the surf zone is composed of the connections between cross shore and along shore currents. Nonuniform bathymetry in the surf zone can lead to the formation of strong cross shore currents, known as bathymetric rip currents [*MacMahan et al.*, 2006; *Moulton et al.*, 2017]. Cross shore currents can also occur on short time scales, known as transient rip currents, and are not related to bathymetry but rather just the wave forcing

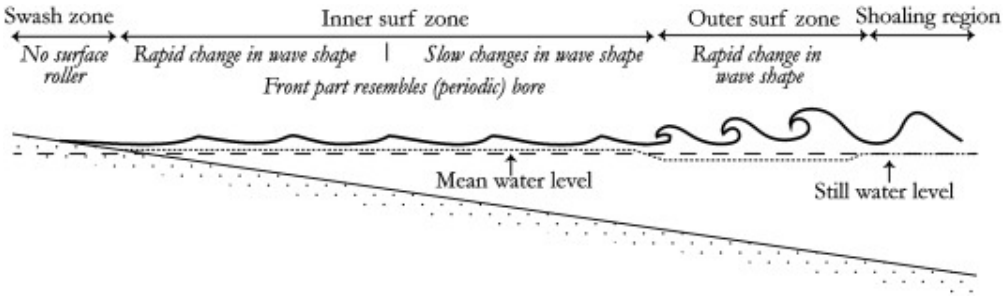

Figure 1.1: Dynamically distinct regions of the nearshore environment on a typical beach. Schematic from [*Jackson and Short*, 2020].

[*Johnson and Pattiaratchi*, 2004]. Along shore currents can be driven by large scale spatial patterns of wave breaking due to the local bathymetry [*Longuet-Higgins and Stewart*, 1964]. The composition of along and cross shore currents results in circulation patterns in the surf zone that can be highly variable both topologically and in intensity [*Moulton et al.*, 2017]. These circulation patterns that form in the surf zone are responsible for the transport of scalars around the surf zone as well as on and off shore [*PINEDA et al.*, 2007]. Many of these near shore processes including turbulence, currents, circulation, and geomorphology changes are all due to wave transformation and breaking processes making wave transformation a crucial process to understand. In this study, we will be mostly focused on measurements waves and currents from the shoaling zone through the inner surf zone but not including the swash zone.

1.0.2 Wave Transformation and Wave Breaking in the Surf Zone

Surface gravity waves are generated by wind stress on the surface of the ocean[*Ursell*, 1956]. These waves radiate outwards from their generation site transporting energy and momentum towards the shorelines. In deep water, a series of random waves have a wave height distribution that follows a Rayleigh distribution [*Longuet-Higgins*, 1980]. As waves move into shallow water they steepen. The process of wave steepening is known as shoaling and is due to the conservation of energy flux. As waves reach shallow water, they interact with

the bottom and the wavelength begins to shorter, as the front of the wave slows relative to the back of the wave. This causes the height of the waves and their steepness to increase to conserve energy. As waves propagate through the surf zone, energy is transferred to high frequency components through nonlinear interactions thus further steepening the waves [*Herbers et al.*, 2000]. Eventually, the waves become too steep, become unstable, then break. As waves break, the distribution of wave heights moving towards shore still remains Raleigh distributed; however, there is energy loss from the larger waves [*Thornton and Guza*, 1983].

Wave breaking is defined as the sudden transition of particle motion in the waves from irrotational to rotational and when the waves begin to lose energy [*Basco and Asce*, 1985]. The process of wave breaking takes organized wave motion and transfers it to multi-scale motion including small-scale turbulence and large-scale mean currents [*Melville*, 1996]. Wave transformation describes the changes in height, shape, length, and other characteristic properties as the waves travel towards the beach through progressively shallower water. Wave transformation includes shoaling and breaking processes. Wave transformation is important to understand to improve our understanding of surf zone processes, especially during extreme events [*Melville*, 1996; *Perlin et al.*, 2013]. Within wave transformation, the least understood parts are the onset of wave breaking and the energy dissipated in breaking [*Barthelemy et al.*, 2018].

Wave transformation is directly controlled by the local bathymetry [*Thornton and Guza*, 1982]. From the connection between the waves and the bathymetry an obvious dimensionless parameter can be created as the ratio of a characteristic wave height to relative water depth referred to as γ defined in equation 1.1.

$$\gamma = H/d \tag{1.1}$$

Where H is a characteristic wave height and d is the local mean water depth. In deep water, γ is very small. As waves enter shallower water this value increases due to both wave height increases from shoaling and water depth decreases. The next obvious question is what is the limiting value of γ and is this value universal. One of the earliest estimates

from [*McCowan*, 1894] suggests that that the limiting value is 0.78 for a solitary wave. This is the general rule of thumb used by most people in the coastal engineering industry [*Galvin*, 1972]. When studied in the field, values ranged from 0.25 to 0.6 depending on beach slope and wave conditions in the mid to inner surf zone, where the characteristic wave height was a significant wave height [*Raubenheimer et al.*, 1996]. When the root-mean-square wave height from a sea surface elevation time series is used, a maximum value of 0.42 was found for γ within the inner surf zone [*Thornton and Guza*, 1982]. When waves reach the maximum value for γ, we assume that they break and begin to dissipate energy. As waves continue to travel towards the shore after reaching a maximum value of γ we assume that the wave height is then reduced linearly with the water depth following the same relationship in equation 1.1 [*Thornton and Guza*, 1982]. This linear reduction is known as saturation since γ reaches a maximum value and then is assumed to stay at this maximum, saturated value as the waves continue towards the beach.

Th energy in a wave scales with the wave height squared, shown in equation 1.2.

$$E = \frac{1}{8}\rho g H^2 \tag{1.2}$$

Where E is the wave energy, ρ is the water density, g is gravitational acceleration, and H is the wave height. From the time the wave starts to break to when it reaches the shoreline, all of the energy contained in the wave is transferred into turbulence, currents, and other processes. If the surf zone is saturated, meaning γ is constant inside the surf zone, we can then know the energy everywhere in the surf zone just by knowing the local depth. This is ideal for use in operational wave models since it is easy to compute everywhere in the model. Within the inner surf zone, in water deeper than 0.8 m, observed values of γ ranged from 0.2 to 0.4 with approximately even spread in this range for variously sloped beaches [*Raubenheimer et al.*, 1996]. While in shallower water, less than 0.8 m, values were seen to range from 0.4 to 0.6 [*Raubenheimer et al.*, 1996]. This change in value even within the inner surf zone raises the question of whether or not the surf zone is truly saturated and how universal the γ parameter really is. However, it has been shown that a one-dimensional, cross shore

energy balance in combination with the assumption of an energy saturated surf zone both qualitatively and quantitatively describes wave transformation compared to measurements in the surf zone [*Battjes and Janssen*, 1978]. The simple cross shore energy balance from [*Battjes and Janssen*, 1978] is shown in equation 1.3.

$$\frac{\partial P_x}{\partial x} + D = 0 \tag{1.3}$$

Here the P_x is the cross shore component of energy flux per unit length and D is the dissipated power per unit area. This balance suggests that all incoming energy flux from the waves is directly balanced by the dissipation through wave breaking. In the field, estimates of energy dissipated in a breaking wave require multiple measurements of individual wave heights and periods [*Carini et al.*, 2015]. From these multiple measurements an estimate of the wave energy flux gradient can be computed which is directly related to the energy dissipation [*Carini et al.*, 2015]. Some studies investigated wave breaking strength, which is directly connected to the energy dissipation, through directly measured accelerations from surface drifters[*Brown et al.*, 2018].

The transition region from the shoaling region to the surf zone is very poorly understood [*Perlin et al.*, 2013]. Wave breaking is an intermittent process which makes measurements of the process challenging, at best. The intermittency and wave-resolved nature of wave breaking also makes it challenging to incorporate energy dissipation directly into wave-averaged wave models which tend to be used as operational forecast models. Recent theoretical, numerical, and laboratory studies have investigated a normalized energy flux to predict the onset of breaking without relying directly on the local water depth. The normalized energy flux is defined in 1.4 [*Derakhti et al.*, 2020]; [*Barthelemy et al.*, 2018].

$$B = \frac{\mathfrak{F}}{Ec} \xrightarrow{At\,Free\,Surface} U/c \tag{1.4}$$

Here, B is the normalized energy flux per unit volume, $\mathfrak{F}$ is the local flux of energy, E is the energy in the wave, c is the wave celerity. At the free surface, this expression condenses to the ratio of the particle velocity at the crest, U, relative to the wave celerity [*Derakhti*

et al., 2020]. It has been theoretically postulated that when the normalized energy flux, B, surpasses a value of 0.85 waves will break and this has been verified numerically and in laboratory settings ([*Barthelemy et al.*, 2018]; [*Derakhti et al.*, 2020];[*Saket et al.*, 2017]). However, this has not been tested in the field especially in large, stormy conditions. This breaking onset criteria also is a wave-resolved phenomena; therefore, in order for this to be used effectively in operational models, a connection needs to be made to wave-averaged waves models. To test these parameterizations and hypothesis' we need measurements that have a high spatial and temporal resolution in a large range of conditions.

1.0.3 Surf Zone and Wave Buoy Measurements

Wave buoys are key instruments for studying ocean surface waves and currents; however, in the past they have been thought to be less accurate for measuring waves than fixed instrumentation [*Collins et al.*, 2014; *Dysthe et al.*, 2010]. While other fixed instrumentation such as pressure gauges and acoustic sensors have been seen to be more accurate than wave buoys, the fixed instrumentation is limited in the conditions it can be deployed in, the amount of instruments deployed, and they are susceptible to damage due to the harsh environment of the surf zone. Due to these limitations, wave buoys become the best option for studying a wide variety of sea states with specific emphasis on extreme events. Early wave buoys were accelerometer based, included roll-pitch-tilt sensors and generally data from the buoys was used to compute scalar and directional energy spectra through standardized procedures [*Kuik et al.*, 1988]. This approach is highly effective for computing spectral estimates, but it does not provide any information about specific waves or the wave time series. The next generation of wave buoys focused on using GPS velocity based processing methods to measure wave spectra and bulk parameters which facilitated smaller scale and more cost effective wave buoys [*Thomson et al.*, 2018; *Herbers et al.*, 2012]. The GPS based processing methods have been impressively effective at measuring deep water ocean waves; however, they are limited to measuring deep water waves due an implicit assumption of circular wave orbital motion [*Thomson*, 2012]. GPS velocity based wave buoys were also used as their

earlier counterparts to investigate waves in a spectral framework rather than a wave-by-wave framework.

Free-drifting, SWIFT (Surface Wave Instrumentation Floats with Tracking) wave buoys have also been used to measure turbulence [*Thomson*, 2012], wave-ice interactions [*Thomson et al.*, 2016; *Rogers et al.*, 2016; *Smith and Thomson*, 2019] and wave-current interactions [*Thomson and Rogers*, 2014] in wave following reference frames. SWIFTs have been used to quantify breaking severity of individual waves [*Brown et al.*, 2018]. The company *SOFAR ocean* has since developed the Spotter buoy that is using a GPS based wave measurement. Many Spotter buoys are being deployed all over the world to create a global network of wave measurements used to model the global wave climate and assist with many industries that rely on accurate measurements and forecasts of waves [*Raghukumar et al.*, 2019].

Few wave buoys have been used in the surf zone to investigate waves. Even fewer studies have tried to combine the power of individual wave buoys to create large coherent arrays. GPS based drifters have been used to investigate surf zone dispersion and circulation patterns [*Schmidt et al.*, 2003, 2005; *Spydell et al.*, 2007]. In the following sections, we will first discuss the development of a new wave buoy called the microSWIFT, the deployment of the buoys, creation of a large dataset and the utility of that dataset for studying inner shelf and surf zone waves.

Chapter 2

METHODS

In this project, we measured waves in the inner shelf and surf zone using coherent arrays of small-scale, free-drifting wave buoys called microSWIFTs. We created an open source dataset of in-situ measurements that has both high spatial and temporal resolution for short intermittent bursts, referred to as missions, lasting between 5 minutes to multiple hours. The microSWIFT buoys measure the kinematics of the sea surface through the use of an inertial measurement unit (IMU) and GPS sensor that are "strapped-down" to the microSWIFT. In this context, coherent arrays refer to multiple buoys that are deployed simultaneously. The direct measurements from the buoys are accelerations, rotation rates, and heading in the reference frame of the buoy along with horizontal velocities and overall position in the earth reference frame. The difference between the body reference frame of the buoy and the earth reference frame is shown in Figure 2.1. Through post processing, the accelerations are corrected to the earth frame of reference and integrated, yielding accelerations, velocities and positions in the earth frame of reference. These measurements are then then converted to a local Cartesian coordinate system so that the measurements can be directly compared with other instrumentation and are physically meaningful. The field site for these measurements is the US Army Corps of Engineers Field Research Facility (FRF) on the Outer Banks of North Carolina, USA. The following subsections will describe the details of how the microSWIFT wave buoys were developed including sensor specifications, hardware and software design, details of the field experiment, post-processing, data cleaning and uniform processing, acceleration measurement correction, data evaluation, and deployment methods.

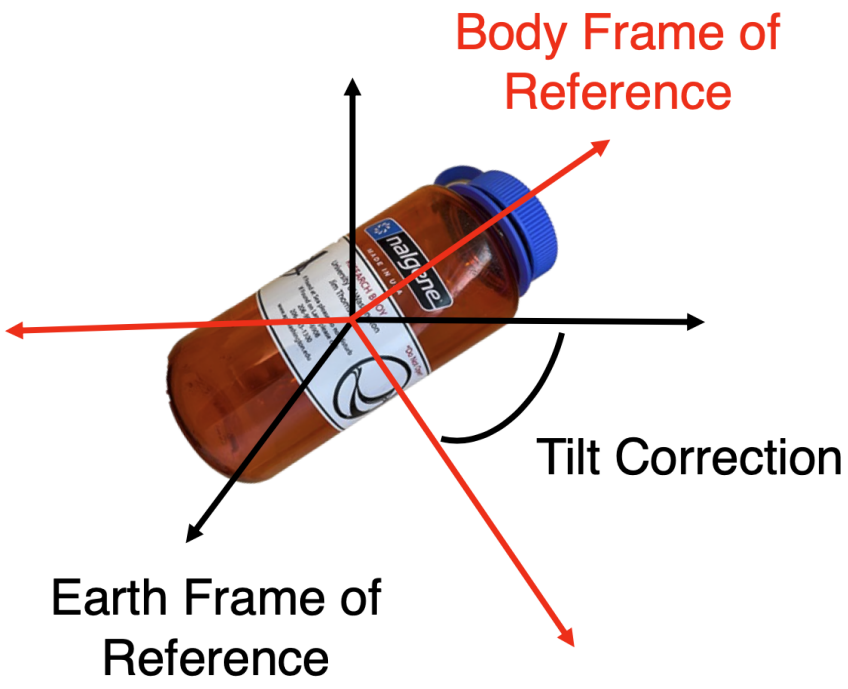

Figure 2.1: Schematic of rotating the body frame of reference to the earth frame of reference of the microSWIFT buoy.

2.1 Development of the microSWIFT Wave Buoy

The microSWIFT wave buoy is a small-scale, low cost, free-drifting wave buoy. The hardware components of the microSWIFT are shown in Figure 2.2. The microSWIFT is an extension of the original SWIFT (Surface Wave Instrument Float with Tracking) that is described in *Thomson* [2012]. The electronics and sensors of the microSWIFT are housed inside of a Nalgene brand water bottle with a length of approximately 21 cm and a diameter of 9 cm. The bottle sits on its side in the water giving a keel of approximately 4.5 cm and a sail of 4.5 cm. The overall microSWIFT has a mass of approximately 0.7 kg. The microSWIFT is powered by two rechargeable lithium-iron D-cell batteries and has an approximate lifespan of 48 hours under the current operating configuration. The instruments on board the microSWIFT are a GPS module and Inertial Measurement Unit (IMU). The entire system is controlled by a Raspberry Pi Zero, a small microprocessor, and has a full Ubuntu Linux operating system. The microSWIFT also has an iridium modem (RockBLOCK 9603) onboard that is used to send processed data from the microSWIFT to a shore-side server. Each component of the microSWIFT is soldered directly onto a custom circuit board as shown in Figure 2.2.

All software for the microSWIFT is written in the Python computing language and is published on a public Github repository for open source access (https://github.com/alexdeklerk/microSWIFT). The flow of onboard software is shown in Figure 2.3. The microSWIFT is controlled by one main function named *microSWIFT.py* that controls all other functions. Once the microSWIFT is turned on, a service script named *microSWIFT.service* is run immediately that starts running the main *microSWIFT.py* control function. Once *microSWIFT.py* starts, it creates a log file where all functions onboard the microSWIFT are logged so the user can see if any errors are occurring or if the instrument is working properly. The microSWIFT main control is split into two windows, the record and process/send windows, that have user defined lengths based on universal coordinated time (UTC) where the user can define when they want a record window to start and how long they want it to be as well as how long they want the process/send window to be. Within the record window,

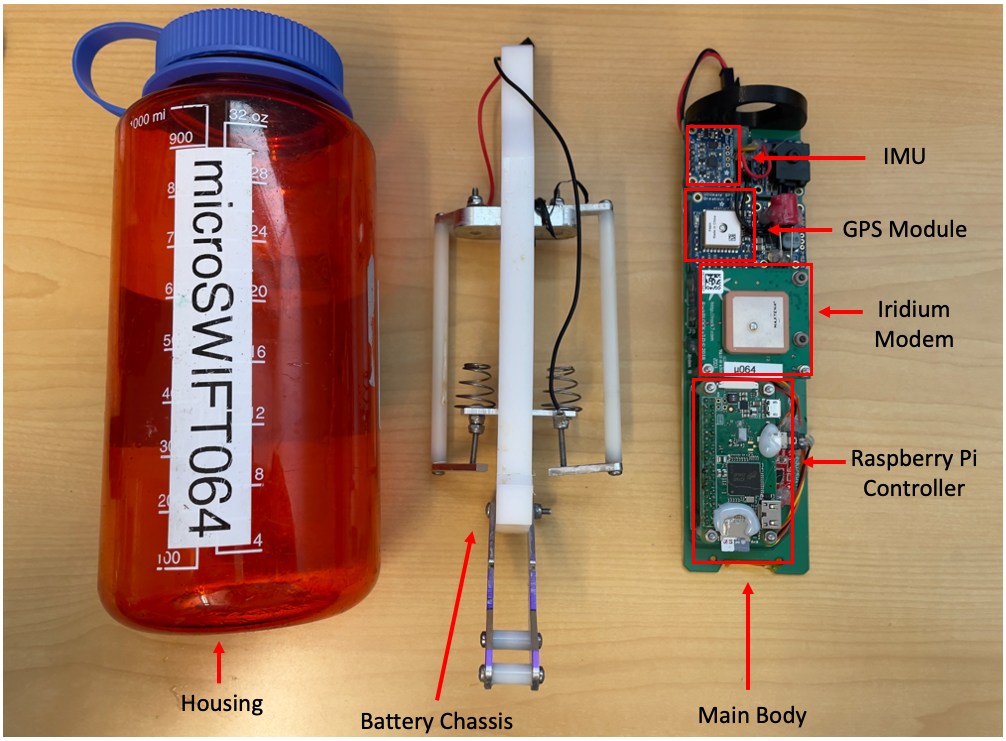

Figure 2.2: Layout of microSWIFT hardware components with the Nalgene water bottle housing on the far left, battery chassis in the middle and the electronics on the far right. The individual chips include a Raspberry Pi Zero as the main processor, a GPS module, inertial measurement unit(IMU) that contains accelerometers, gyroscopes and magnetometers and an iridium modem.

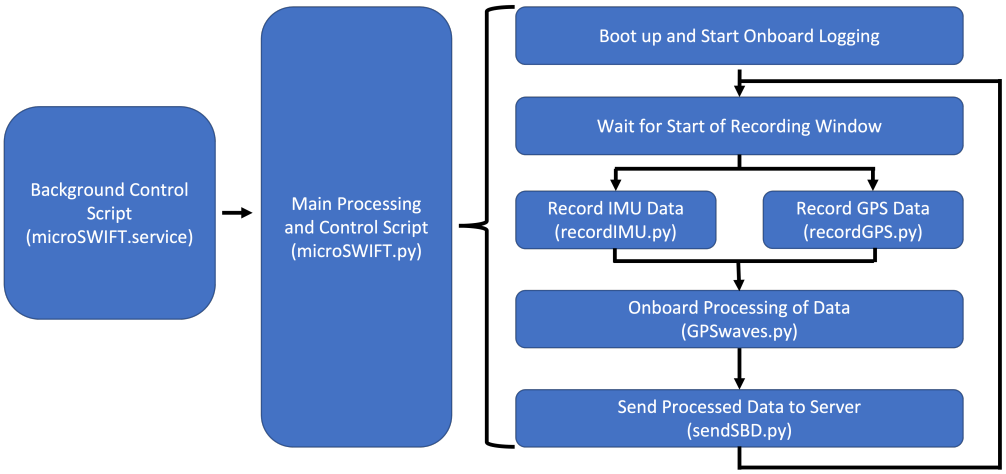

Figure 2.3: Software onboard the microSWIFT and flow of operations.

the microSWIFT creates two "futures" which are functions that will run concurrently onboard the microSWIFT and will appear to be effectively parallel functions but are not truly parallelized since there is only one processor onboard the microSWIFT. The functions that are run concurrently are used to record the GPS measurements and IMU measurements and are named *recordGPS.py* and *recordIMU.py*, respectively. These functions end at the end of the user defined record window and then the microSWIFT enters the process/send window.

Within the process and send window, the microSWIFT reads in all of the recorded GPS velocities and uses the algorithm *GPSwaves* described in *Thomson* [2012] to compute an estimate of the wave energy scalar spectrum, bulk parameters, last known location, and the average north-south and east-west velocities over the length of the last record window. These processed values are then packaged into a binary message that is sent through the iridium modem to a shore-side server where the data can be parsed and used. If the data that is processed from each window cannot be sent through the iridium network during the send window, it is added to a queue that will attempt to send the data at the next send window. The onboard processing and iridium network functions of the microSWIFT were not heavily used in this project due to limitations in the processing method. The *GPSwaves* algorithm is very effective for deep water waves and uses an assumption of circular wave orbital velocities

to estimate the scalar energy spectrum. However, this assumption is violated in shallow water due to the non-linearity of nearshore waves. To remove this assumption, we developed a new processing method that will be described in detail in the following sections. While the onboard processing and iridium network usage was not crucial for this project, it will be crucial for other projects that use the microSWIFT in situations that the buoy may not be recovered such as to study hurricanes or waves in ice in the future.

The GPS module uses the MT3339 chipset. The GPS samples at a rate of 4 Hz and reads direct national marine electronics association (NMEA) strings. Onboard the microSWIFT, all of the raw NMEA strings are saved directly. In the post processing, we read in the GPGGA and GPVTG NMEA strings, which give measurements of the global position (latitude and longitude), altitude, speed-over-ground, and course-over-ground. The course-over-ground is used to decompose the speed-over-ground into east-west and north-south velocity components. The inertial measurement unit (IMU) onboard incorporates an accelerometer, gyroscope, and magnetometer. Each sensor measures in three orthogonal spatial dimensions. The IMU samples at a rate of 12 Hz. The specifications for the IMU are stated in Table 2.1.

Throughout this experiment, the microSWIFT was configured to begin recording at the start of every hour then stop recording at minute fifty of the hour, process the recorded data, and send it to the shore-side server through the iridium network from minute fifty to the start of the next hour. This configuration was useful to get bursts of data and check the location of each buoy; however, it led to some deployments that have ten minute gaps in the middle of them. As described in the following sections, the deployment operations were aware of this limitation and it was planned for accordingly.

2.2 Field Experiment - During Nearshore Events Experiment (DUNEX)

This project is part of a larger collaborative project named DUNEX(During Nearshore Events Experiment) that is funded through the US Coastal Research Project (USCRP, https://uscoastalresearch.org). The goal of the overall project is to further investigate the effects of storm events on the coastal environment. Our specific goal was to understand

Sensor	Chipset	Sensitivity	Range	Average Noise Variance
3-axis Linear Accelerometer	FXOS8700CQ	0.244 mg/LSB 0.488 mg/LSB	$\pm 2g / \pm 4g$	0.00004 ms^{-2}
3-axis Magnetometer	FXOS8700CQ	0.1 $\mu T/LSB$	$\pm 1200 \mu T$	2 μT
3-axis Gryoscope	FXAS21002C	15.625 mdps/LSB	$\pm 500 dps$	0.045 dps

Table 2.1: Inertial Measurement Unit sensor specifications for accelerometer, gyroscope and magnetometer onboard each microSWIFT. Note that the dynamics range of the accelerometer was adjusted from 2g to 4g part way through the field experiment on Mission 53 on October 23rd, 2021.

the dynamics of wave transformation and circulation patterns in a large variety of forcing conditions from ambient up to extreme conditions. During October 2021, a 27-day field campaign was held from October 3rd to October 30th where coherent arrays of microSWIFTs were deployed daily into the nearshore environment. The site of this field experiment was the US Army Corps of Engineers Field Research Facility in Duck, North Carolina, USA. The bathymetry at the field site was surveyed regularly throughout the experiment. An example of the measured bathymetry is shown in Figure 2.4. Here, we see a large channel at approximately 500 meters in the along shore direction extending from the beach offshore which is due to scour around the pier that is at the field site. We also see the presence of a large, shore-parallel sandbar at approximately 200 meters in the cross shore direction, which leads to unique and interesting hydrodynamics at this site. The locations of the fixed instrumentation are also shown in Figure 2.4. All of the fixed instrumentation was on the north side of the pier.

In this experiment, coherent arrays will be defined as a set of multiple buoys that are

deployed in the water and measuring simultaneously as they drift through the surf zone. Each coherent array is referred to as a "mission". The descriptions of each mission deployment are shown in Appendix A. The microSWIFTs were deployed by personnel swimming them out on surfboards, thrown from the FRF pier, taken out on jet-ski by local lifeguards, and dropped from a helicopter. It is important to note that the microSWIFTs deployed from the helicopter had parachutes attached and therefore behave differently in the water. Many of the missions lasted approximately 20 minutes while some were shorter and few went longer than an hour with all mission duration's and deployment methods noted in Appendix A. A total of 81 missions were completed during the course of the field experiment. During each mission, we relied on "shepherd buoys" which are buoys that are ballasted the same way but instead of the microSWIFT electronics the were equipped with a Garmin brand dog tracking collar (T5 mini) which gave us a real-time location of some of the buoys so we could figure out general circulation patterns during operations and recover the buoys. Including the "shepherd buoys," 2,187 individual buoy deployments were completed during the experiment. Some of the missions were too short or were unusable for various reasons. These unusable components were removed in a data cleaning process. All data cleaning notes have been listed in Appendix B. After data cleaning, 73 missions with 1,154 individual microSWIFT tracks remained as reliable measurements.

Along with the coherent arrays of microSWIFTs, fixed instrumentation at the field site included rectified imagery, water level gauges, offshore wave buoys, bottom mounted acoustic wave and current (AWAC) sensors and high resolution bathymetry surveys conducted by the FRF. A map showing the location of the fixed instrumentation and the bathymetry of the field site during the experiment is shown in Figure 2.4. The fixed instrumentation is crucial to add context to the measurements from the microSWIFT arrays and was used operationally and for analysis. The fixed instrumentation is also used to validate the measurements from the microSWIFT arrays. The tracks of all microSWIFTs deployed over the experiment are plotted over the surveyed bathymetry are shown in Figure 2.5. The buoy measurements cover a significant portion of the field site and cover the transition from the nearshore region

to the surf zone. The data collected from each microSWIFT and how it is organized, cleaned, and processed is discussed in the following section.

2.3 Computation of Sea Surface Elevation

The microSWIFTs measure accelerations in the body reference frame of the drifting buoy and are agnostic to which direction is meaningful to us on earth. To make these measurements meaningful, they must be corrected to be in the reference frame of the earth. A schematic of the rotation from the body frame to the earth frame of reference is shown in Figure 2.1. Here we see that as the buoy moves through the water, the mapping from the body reference frame to the earth reference frame is always changing and requires a tilt correction estimated at each step to correct these accelerations. There are many different methods to correct accelerations with varying degrees of complexity. This section will review the methods that were explored in this analysis and the assumptions and limitations behind each method. The method with the most skill is was found to be an 9-axis indirect Kalman filter for fusing IMU data and is prepackaged in the MATLAB Navigation toolbox. The most important acceleration for us to correct was the vertical acceleration, which would then be integrated to estimate sea surface elevation and vertical velocity, which are crucial for studying surface gravity waves. The horizontal accelerations are less crucial especially since we have direct measurements of horizontal velocities from the GPS unit that are already within the earth frame of reference.

2.3.1 Creation of Test Dataset

Prior to testing any method, a test dataset was created from a subset of the DUNEX dataset to compare how well the computed scalar wave spectrum and bulk wave parameters compared with "ground truth" measurements. The data subset consists of any microSWIFTs that were in a location where the water was between 4-5 meters deep, continuously for at least 10 minutes, based on the GPS location of the microSWIFTs and the bathymetric survey that is published from the FRF and as shown in Figure 2.4. The sea surface elevation was then computed from each method and a scalar energy spectrum was computed directly from

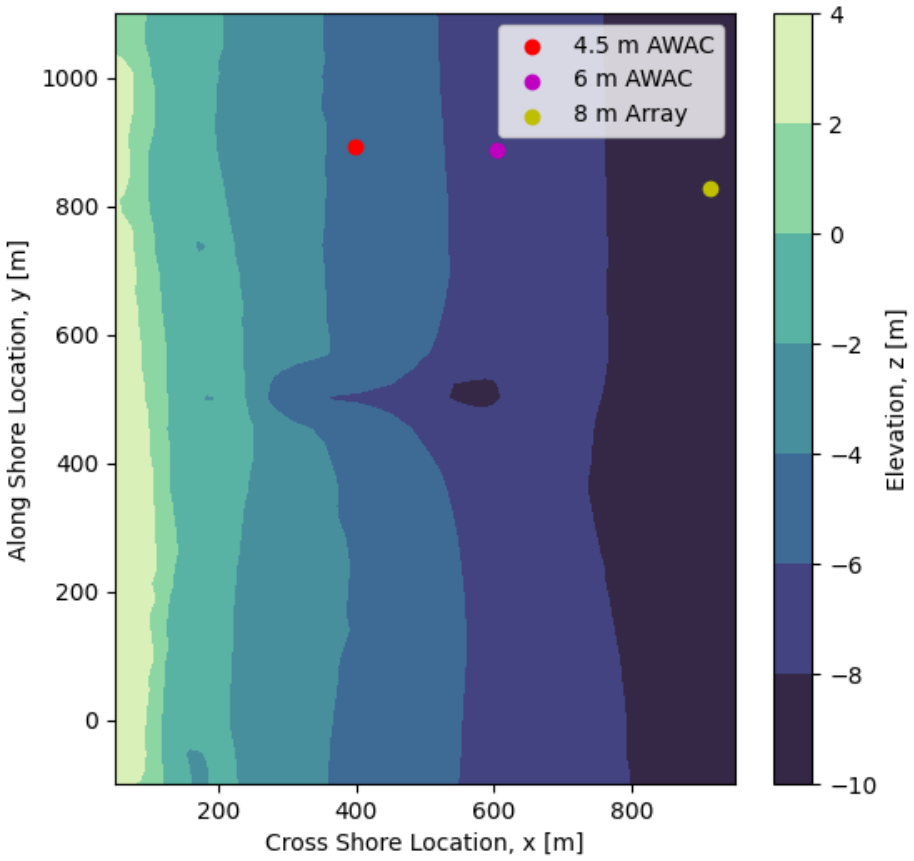

Figure 2.4: Representative surveyed bathymetry digital elevation model at the Field Research Facility from October 21st, 2021 relative to NAVD88 and locations of fixed instrumentation.

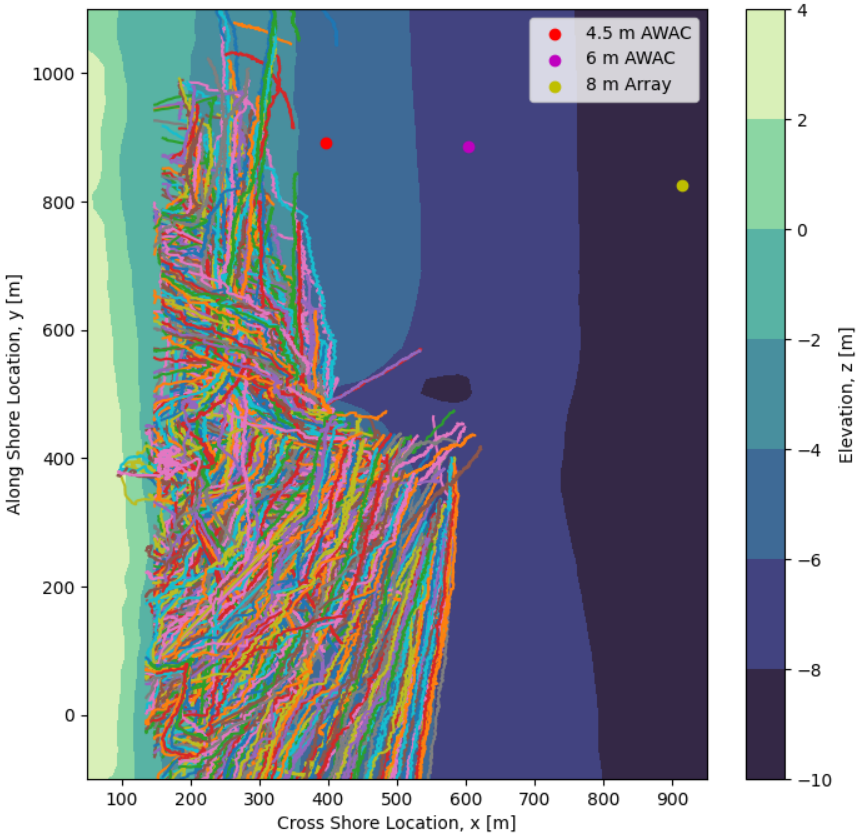

Figure 2.5: Composite map of all buoy drift tracks measured throughout the entire experiment overlaid on representative surveyed bathymetry and locations of fixed instrumentation. We see that the drift tracks cover a huge portion of the field site including the transition between the inner shelf and surf zone. Some tracks continued further south out of the measured bathymetry and are not shown.

the sea surface elevation time series. These spectra were then compared to the spectrum computed from the 4.5 meter AWAC (location shown in Figure 2.4) which was recording for the entirety of the month. The main assumption here is that bathymetry is the main control for the wave transformation and that there is not much along shore variability within the domain of the FRF. Note that this depth did not need to be corrected for mean sea level since the seafloor elevation of the 4.5 meter AWAC and the bathymetry are both relative to the same datum. While we are assuming that there is not much along shore variability in the waves statistically, this is a question that we would like to further investigate in the future but was a necessary assumption to create this validation dataset. While the AWAC measurements are measurements as well and also have errors, it has been an established instrument and will act as the ground truth for this analysis.

2.3.2 General Processing Methods

A flow chart of the all the processing methods is presented in Figure 2.6. The general computation method and comparison consists of six steps. The first step is getting the raw measurements from the microSWIFT while it is deployed in the water. The second step is correcting the accelerations from the body frame to the earth frame of reference through an orientation estimation algorithm, which will be discussed in much more detail in the following section. The third step is filtering the corrected signals with a band-pass, first order Butterworth digital filter with high and low frequency cutoffs of 0.05-0.5 Hz (filtering outside of the surface gravity wave frequency band), respectively. In step four, the filtered accelerations are integrated via a time domain cumulative trapezoid method to velocities. In step five, the velocities are filtered again with the same filter to eliminate any spurious integration errors and integrated to positions then filtered one last time. The sixth and final step is computing a scalar energy from the vertical position time series. The scalar energy spectrum is computed directly from the time series via Welch's method with Hanning windows that are 300 seconds (3600 points) and 50% overlap of windows. Each five adjacent spectral estimates are then band averaged to improve the statistical significance of each

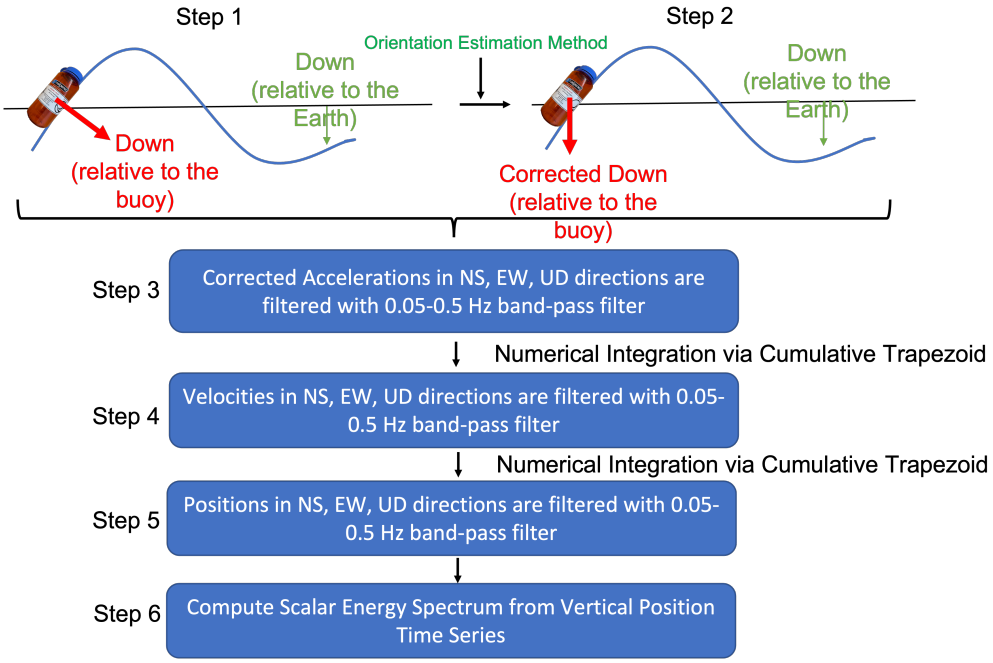

Figure 2.6: Flow of microSWIFT data post-processing methods from the raw IMU measurements through the computation of a scalar energy spectrum.

estimate. These spectral characteristics create spectra with a minimum of 54 degrees of freedom. Similar to the 48 degrees of freedom for scalar spectrum computed from 4.5 m AWAC. The significant wave height is computed directly from the scalar energy spectrum along with the peak period. The scalar energy spectrum, significant wave height, and peak period are then directly compared to the estimates from the 4.5 m AWAC. The correction method that most closely agreed with the 4.5 m AWAC estimates was chosen as the highest performing method and applied to the remaining dataset.

We compared no correction, which was the baseline estimate, to two correction methods to see how well the correction methods improved the results relative to the 4.5 m AWAC. The two correction methods that we explored fully were a 9-axis extended Kalman filter for IMU fusion and a 9-axis indirect Kalman filter for IMU fusion. The no correction method was based on the assumption that, on average, the microSWIFT is stable in the water so the

vertical acceleration measured aligns with the true vertical acceleration in the earth frame of reference. This assumption is reasonable since the mean value of the measured vertical accelerations is centered around approximately 9.8 ms^{-2}, the gravitational acceleration. However, we also see visually that the microSWIFT rolls in the water, referred to as the "twitch", which could contaminate the measurements with spurious, non-physical motion. Both correction methods were types of Kalman filters that fused data from the IMU in slightly different ways.

2.3.3 Orientation Estimation and Kalman Filter Basics

The orientation of the buoy is a dynamic variable and the time evolution of the orientation is modeled as a dynamical system [*Labbe*, 2014]. The orientation or heading of the buoy in 3D space can be described by a four dimensional quaternion, that we will refer to as q, as defined in equation 2.1.

$$\vec{q} = [q_1, q_2, q_3, q_4] \tag{2.1}$$

A quaternion is a compact and efficient way to describe the mapping of one vector to another. As we saw in Figure 2.1, we are wanting to map the acceleration vector from the body frame of reference to the earth frame of reference at every time step. This mapping is described in equation 2.2.

$$\begin{bmatrix} A_x \\ A_y \\ A_z \end{bmatrix} = R(\vec{q}) \begin{bmatrix} a_x \\ a_y \\ a_z \end{bmatrix} \tag{2.2}$$

In this mapping, the lowercase a values are the body frame of reference accelerations that are being mapped the earth frame of reference accelerations defined as the uppercase A components. This mapping is linear and easy; however, the map $R(\vec{q})$ is not known and changes at every time step as the buoy's orientation changes. Therefore, to correct these accelerations we must solve for the the orientation $\vec{q}$. While at first this may seem simple,

we do not have a fully determined system. If we could directly measure the roll, pitch, and yaw of the buoy we could easily find the mapping. However, we only measure the rotation rate and the starting orientation is unknown. Therefore, we must estimate the orientation at each time step by combining multiple pieces of information to best estimate the overall state of the system. The state-of-the-art way to get the best estimate of a state is through the use of a Kalman filter.

A Kalman filter is an estimation technique that uses multiple sources of information, such as multiple sensors or physical models, to estimate a state variable of interest [*Kalman*, 1960]. In this context, the state variable we are trying to estimate is the orientation of the buoy in the earth reference frame. All Kalman filters are composed of two fundamental steps, the prediction step and the correction step [*Kalman*, 1960]. In a basic Kalman filter, the prediction step can be written as 2.3 from *Kalman* [1960] (adapted from the documentation found at https://ahrs.readthedocs.io/en/latest/filters/ekf.html).

$$\hat{\vec{x}}_t = F\vec{x}_{t-1} \tag{2.3}$$

Here $\hat{\vec{x}}$ is the predicted system state at time t, F is a model function to predict the state of the system at the next time from the previous time, and $\vec{x}_t$ is the state of the system at the previous time step. The next step in a Kalman filter is the correction step that is written in equation 2.4 also from *Kalman* [1960].

$$\begin{aligned} \vec{v}_t &= \vec{z}_t - H\hat{\vec{x}}_t \\ \vec{x}_t &= \hat{\vec{x}}_t + K_t\vec{v}_t \end{aligned} \tag{2.4}$$

Here, we are first computing the measurement residual, $\vec{v}_t$, from the predicted state, $\hat{\vec{x}}_t$, an observation model, H, and an actual measurement of the system, $\vec{z}_t$. From this measurement residual, we can correct the predicted state using a Kalman gain factor K and the predicted state. How the Kalman gain factor is computed will be left to reader to further explore the literature starting with *Kalman* [1960].

These steps are ubiquitous to all Kalman filters; however, the ways in which these steps are carried out varies between systems. In the problem of estimating the orientation of a rigid body in space, as is our case, the equations that model the measurements are nonlinear [*Sabatini*, 2011]. In order to handle the nonlinear measurement model equations multiple techniques and types of filters have been developed. The Kalman filters explored in this study were an extended Kalman filter and an indirect Kalman filter . The extended Kalman filter estimates the orientation of the buoy directly and linearizes the nonlinear measurement models through the use of Taylor series expansions [*Sabatini*, 2011]. Another approach to handling the nonlinearities is to avoid nonlinear equations and instead model the error of the orientation between the predicted and measured orientation which known as an indirect Kalman filter [*Roetenberg et al.*, 2005]. The extended and indirect Kalman filter approaches have been developed into pre-packaged algorithms in the MATLAB and Python programming languages, respectively. Both algorithms were tested as correction methods in the analysis.

2.3.4 Method Comparisons and Evaluation

Computing the scalar energy spectrum and bulk wave parameters with each correction method, we find that the highest performing correction method is the 9-axis indirect Kalman filter that is packaged within the MATLAB navigation toolbox. An example comparison of scalar energy spectra from each method with estimates from the 4.5 m AWAC is shown in Figure 2.7. In this example, we see some features that are common to different methods. The no correction method and the extended Kalman filter tend to drastically overestimate the energy in the low frequencies. The extended Kalman filter drastically underestimates the energy at the high frequencies and the indirect Kalman filter closely resembles the overall shape of the 4.5 m AWAC spectra but slightly underestimates across all frequencies. The difference between the 4.5 m AWAC spectra and spectra for each correction method was then computed for each test case, which for this analysis we will refer to as the error. These error estimates are then averaged across all of the validation dataset test cases. The errors are assumed to be normally distributed while the confidence intervals of each spectral es-

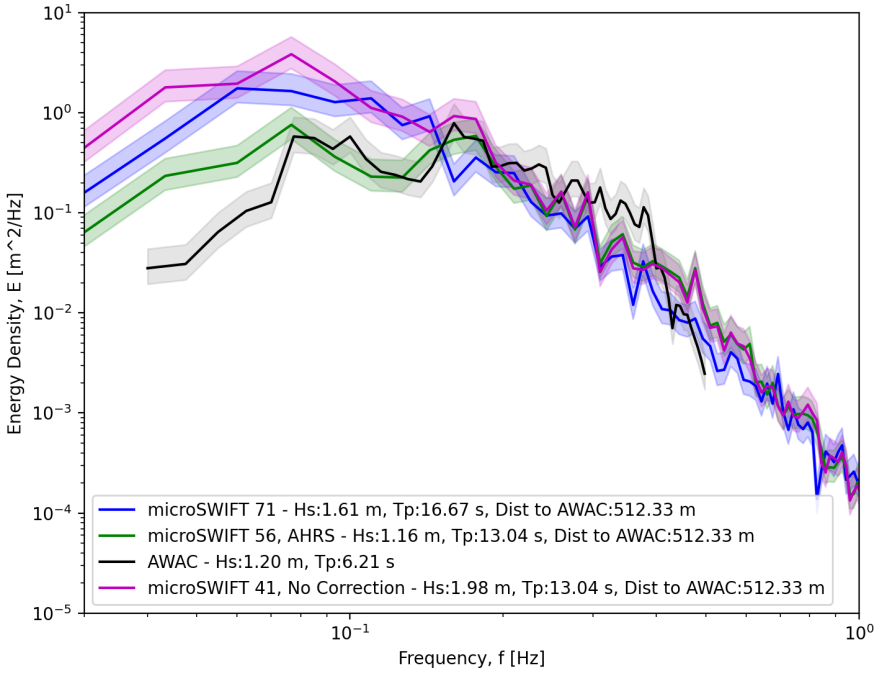

Figure 2.7: Example test case comparison of scalar energy spectra between no acceleration corrections, the extended Kalman filter and indirect Kalman filter with the ground truth 4.5 m AWAC. The semi-transparent filled sections represent 95% confidence intervals around each estimate based on equivalent degrees of freedom and a χ^2 distribution.

timate are χ^2 distributed. From this assumption that the errors are normally distributed, 95% confidence intervals are computed based on the distribution of error at each frequency (Figure 2.8). In this figure, the horizontal line at zero represents "no error" between the estimation method and the 4.5 m AWAC spectra. Here we can see that, on average, the indirect Kalman filter has the lowest error at all frequencies. As we saw in the example, on average, the extended Kalman filter overestimates at the low frequencies and underestimates at the high frequencies, while the no correction method mostly overestimates at the low frequencies.

From each spectrum, the bulk wave parameters are computed and results are shown in

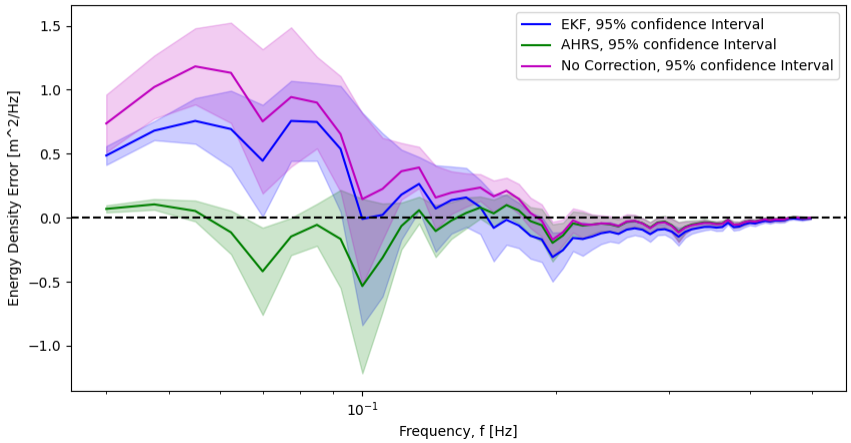

Figure 2.8: Average error of each spectral component computed from each acceleration correction method compared to the 4.5 m AWAC spectra across all thirteen test cases. 95% confidence intervals are shown based on the distribution of errors across all test cases and errors are assumed to be normally distributed.

Table 2.3.4. Again, the error is defined as the difference between the estimate and the ground truth value. Here we see that, on average, the error in the significant wave height between the ground truth and the two correction methods is almost equivalent, where the extended Kalman filter tends to overestimate the significant wave height by approximately 11 cm and the indirect Kalman filter underestimates the significant wave height by approximately 12 cm. These are both drastic improvements from the no correction method that, on average, overestimated the significant wave height by 30 cm. The extended Kalman filter performs best on average for estimating the peak period where it overestimates by 0.99 seconds on average while the AHRS navigation toolbox underestimates by 3.13 seconds and no correction overestimates by 1.44 seconds. Based on these test case comparisons, the highest performing method for estimating the sea surface elevation was the 9 axis indirect Kalman filter for IMU data fusion since it on average across all test cases had the lowest error in the spectra, no strong bias at any frequency band and estimated the bulk wave parameters with high skill.

Correction Method	Average Significant Wave Height Difference [m]	Average Peak Period Difference [seconds]
No Correction	0.31	1.44
Extended Kalman Filter	0.11	0.98
Indirect Kalman Filter	-0.10	-3.13

Table 2.2: Average differences across all test cases between significant wave height and peak period computed from each correction method compared to estimates from the 4.5 m AWAC.

2.4 Deployments, Uniform Processing and Data Products

Deployments of coherent arrays were organized based on a "mission" system where each mission had a defined start time when all microSWIFTs were deployed and an end time when all microSWIFTs were out of the water. The metadata on each mission was recorded by a designated recorder for each mission. The metadata recorded was the start time, end time, number of microSWIFTs deployed, individual numbers of microSWIFTs deployed, the mission number, people deploying, and the method of deployment. Using this metadata, the raw microSWIFT data was organized so that all data on a particular mission was saved together in the same file. After this initial organization, the data from each microSWIFT array is processed uniformly in the following procedure. First, the raw data is read in from text files, parsed, and converted to numeric values. The data measured between the recorded start and end time are saved and the data outside of these times are discarded. The IMU samples at a rate of 12 Hz while the GPS samples at a rate of 4 Hz. Therefore, to have a uniform time array, the GPS values are up-sampled through linear interpolation onto the 12 Hz sampling rate. Linear interpolation was chosen here since it is the simplest method and while we expect smooth continuous motion, we do not want to introduce any spurious data between samples by using a method such as a cubic spline interpolation scheme. Once all data is on a uniform time base, any missing data points from any channel are filled via a

linear interpolation scheme.

Once the data is organized into missions and sorted onto one time array so that it can be indexed uniformly, the dataset is cleaned using a combination of automated and manual methods. First, a spatial threshold is created to remove any data points while a sensor is on the beach. This threshold is created using the bathymetric surveys conducted at the FRF and the mean water level during the mission in question. The mean water level is added to bathymetry to find the instantaneous depth at each surveyed point during each mission. Then the furthest offshore dry point, denoted by a positive depth value, is found and set as the spatial threshold for that mission. An additional buffer of two meters is added to the spatial threshold to ensure that any points offshore of this line are definitely in the water and not rolling on the beach leading to spurious measurements. Any points that then cross this beach threshold are replaced with "NaN" values in the dataset. After this automated cleaning method, all raw data channels were looked through manually and any spurious points are also replaced with "NaN" values. The recorded start and end times of the mission were also adjusted since there were times that the recorded start and end of the mission did not completely correspond to when the microSWIFTs were in or out of the water as seen by large acceleration spikes at the beginning of end of the missions from being deployed or recovered. Depending on the deployment type, the microSWIFTs were sometimes picked up in the middle of the mission, e.g., during jetski based deployments, and therefore those times needed to be removed as well. All data cleaning including start and end time adjustment and individual point cleaning is noted in full in Appendix B. Once the dataset was cleaned and quality controlled, further processing of the data took place. First, all spikes in the IMU measurements were removed using a piecewise cubic Hermite interpolating polynomial (PCHIP) function that is a shape preserving interpolation scheme. The quality controlled IMU variables are then used to correct the accelerations using the 9-axis indirect Kalman filter as discussed in section 2.3.4. From this correction we get time series of accelerations, velocities and positions of each buoy. The global positions are then transformed to the FRF Cartesian coordinate system.

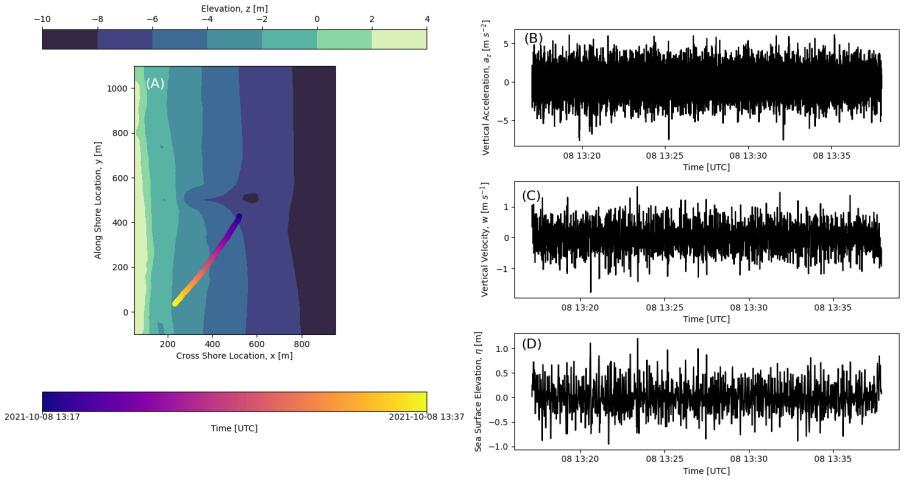

Figure 2.9: Example of some data from a single microSWIFT on one mission. Panel A shows the track of the microSWIFT over the field site bathymetry colored by the time during the mission from the start to the end. Time series throughout the mission of this microSWIFT of vertical acceleration (B), vertical velocity (C) and the sea surface elevation (D) are shown.

After all of the data from each mission has been processed, it is organized and saved as individual netCDF files that can easily be stored, transferred, and analyzed in any major programming language. The description of each data product in every mission file is laid out in Table 2.3. Each variable is available for every microSWIFT on every mission. Some missions have been removed from the dataset along with some microSWIFTs as noted in detail in Appendix B. An example of data from one microSWIFT on one mission is shown in Figure 2.9. Panel A of this figure shows the position of the microSWIFT as it moves through the inner shelf and surf zone in the local Cartesian coordinate system and is colored by the time from the start of the mission to the end in universal coordinated time (UTC). Panels B through D show time series of the vertical acceleration, velocity and position (sea surface elevation) respectively in the corrected earth frame of reference. Similar time series exist for all variables listed in Table 2.3. In the following sections, further validation of this dataset is shown as well as the how this new instrument, deployment technique and correction methods can further be used to study the dynamics of waves in the inner shelf and surf zone regions.

Variable Name	Description	Units
time	date and time in UTC	seconds since 1970-01-01 00:00:00
imu_freq	IMU sampling frequency, single value	Hz
gps_freq	GPS sampling frequency, single value	Hz
accel_x_body	lateral acceleration in the body reference frame	ms^{-2}
accel_y_body	lateral acceleration in the body reference frame	ms^{-2}
accel_z_body	vertical acceleration in the body reference frame	ms^{-2}
accel_x	lateral accelerations in the earth reference frame	ms^{-2}
accel_y	lateral accelerations in the earth reference frame	ms^{-2}
accel_z	vertical accelerations in the earth reference frame	ms^{-2}
gyro_x	rotation rate about the x-axis	dps
gyro_y	rotation rate about the y-axis	dps
gyro_z	rotation rate about the z-axis	dps
mag_x	rotation rate about the x-axis	μT
mag_y	rotation rate about the y-axis	μT
mag_z	rotation rate about the z-axis	μT
u	velocity in the cross shore direction in the local FRF coordinate system	ms^{-1}

Variable Name	Description	Units
v	velocity in the along shore direction in the local FRF coordinate system	ms^{-1}
w	vertical velocity in the cross shore direction in the earth reference frame	ms^{-1}
xFRF	Cross shore location in the FRF coordinate system	m
yFRF	Along shore location in the FRF coordinate system	m
eta	Sea surface elevation in the earth reference frame	m
lat	global position latitude	degrees north
lon	global position longitude	degrees east

Table 2.3: Data products in each mission netCDF file of the DUNEX dataset with descriptions and units. Note that each variable other than time, IMU frequency and GPS frequency is stored within a microSWIFT group and each variable is unique to each microSWIFT.

Chapter 3

RESULTS

3.1 Individual Wave Measurements from microSWIFT Arrays

T he true power of the DUNEX microSWIFT dataset is in deployment of the large coherent arrays. In the previous sections, we discussed how individual microSWIFT measurements were validated against fixed instrumentation; however, individual point measurements in the inner shelf and surf zone have been used in many other studies. Through the use of large coherent arrays, we are able to measure individual waves across large areas of the inner shelf and surf zone simultaneously. By measuring many locations at the same time, the statistics of bulk parameter estimates and spectral estimates are much more robust than from individual measurements. Using the acceleration correction and integration method discussed in the previous chapter, the sea surface elevation time series was computed for each microSWIFT on every mission. From the sea surface elevation time series, a zero crossing algorithm was run across each time series to extract individual waves. The height of each wave, from crest to trough, and average location of the wave was computed. An example distribution of wave heights and average locations is shown in Figure 3.1 from mission 15. Here we see that by combining the measurements from all of the microSWIFTs we are able to get a distribution of wave heights with a very large sample size over a short period of time. From this distribution of wave heights, a significant wave height is computed as the average top one third of the distribution by definition. From *Thornton and Guza* [1983], we expect the wave heights to be Raleigh distributed and that is approximately what we see in the wave height distributions. However, further work will be needed to more quantitatively say how well the wave height distributions agree with a theoretical Raleigh distribution.

This method of estimating a significant wave height was applied to every mission and

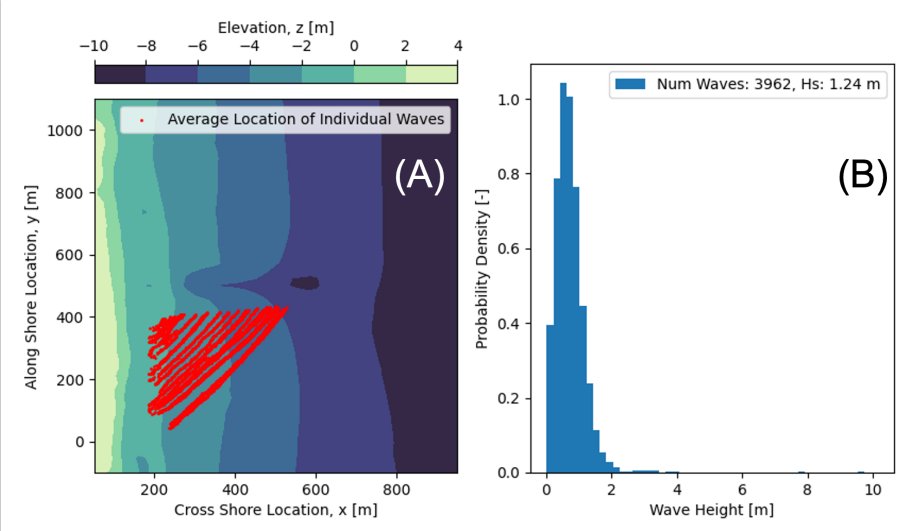

Figure 3.1: Individual waves measured during Mission 15 where panel (A) shows the average location of each wave plotted over the surveyed bathymetry and panel (B) shows the distribution of 3,962 individual waves measured during this 21 minute period through 34 deployed microSWIFTs.

a significant wave height wave was computed for each individual mission in the cleaned dataset. The computed significant wave heights are then shown compared to measurements made by the nearby 4.5 m AWAC over the entire experiment as shown in Figure 3.2. Panel A shows that qualitatively the significant wave heights estimated from the entire microSWIFT arrays agree with the significant wave height from the 4.5 m AWAC across a wide range of forcing conditions. Panel B quantitatively shows that the microSWIFT array estimates of significant wave height agree strongly with the 4.5 m AWAC estimates with a linear regression slope of 1.06, a coefficient of determination of 0.72 and a p-value less than 0.05 suggesting that the significant wave height measurements from the microSWIFT coherent arrays are not statistically different from the AWAC measurements. This finding validates that the microSWIFT arrays are an effective tool to measure individual waves in the inner shelf and surf zone and the coherent arrays are able to accurately measure the significant wave height in the inner shelf and surf zone.

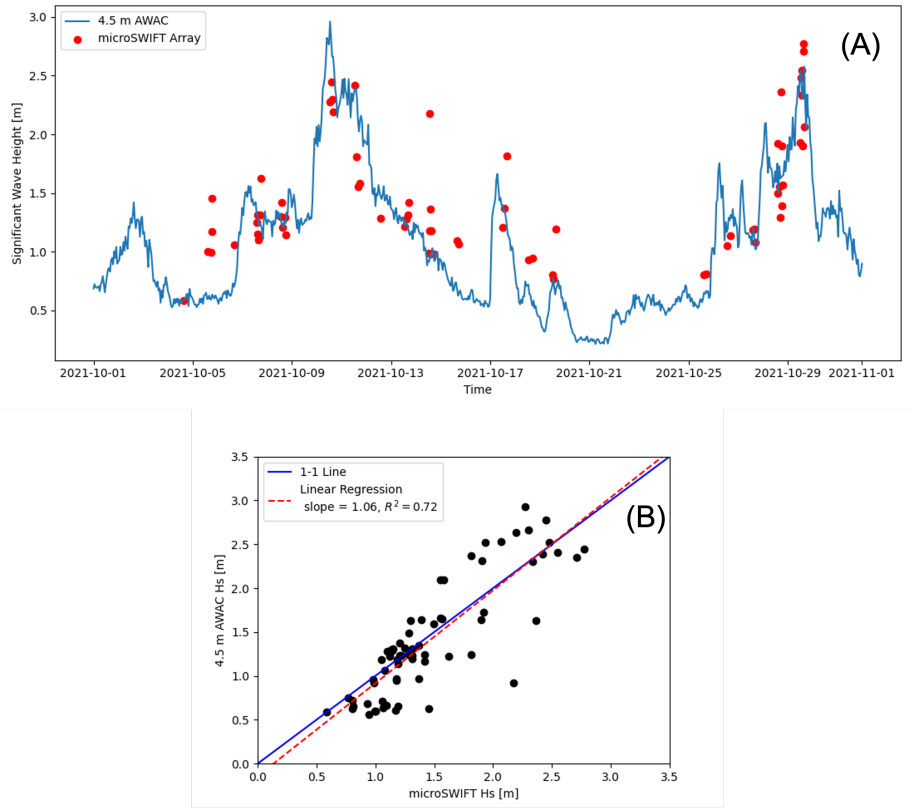

Figure 3.2: Comparisons of estimated significant wave height from the microSWIFT arrays and the 4.5m AWAC through the entire experiment shown as a time series (A) and a direct comparison between measurements (B). We see that the significant wave height estimates from the microSWIFT arrays are not statistically different from the 4.5 m AWAC estimates.

3.2 Wave Transformation Across the Surf Zone Using Coherent Arrays of Drifters

Using these novel microSWIFT coherent array, we are able to investigate the wave transformation from the inner shelf to the surf zone. Across the entire experiment, the height of individual waves was computed as described previously. The wave heights are then normalized by the average depth during each zero crossing interval. These normalized wave heights are then binned into a normalized cross shore location. The cross shore locations are normalized by an estimated surf zone width. The surf zone width is computed from an expected

$\gamma_b = 0.5$ where the wave height is the significant wave height of the mission and the surf zone width is found as the cross shore location where the average depth makes the relationship $H_s = \gamma_b d$ true. The mean value, first and third quantiles of each cross shore location bin distribution are computed and shown in Figure 3.3. Here we see moving from offshore, on the right, to onshore, on the left, an elevation of normalized wave height reaching a maximum value of just over unity at around half of the surf zone width from shore then a sharp decrease in wave height as the waves reach the inner surf zone. The structure of this wave transformation agrees with previous models and field experiments that explain the shoaling of waves and eventually the wave height reduction in the inner surf zone [*Battjes and Janssen*, 1978; *Thornton and Guza*, 1983]. While the shape of the cross shore wave height transformation profile agrees with other studies, the normalized wave heights measured in this study are elevated compared to values found in previous studies [*Raubenheimer et al.*, 1996; *Thornton and Guza*, 1983; *Lenau*, 1966]. This elevation of normalized wave height could be due to skewed locations of waves especially within the surf zone. The location of each wave is based on the average position of the buoy during each zero crossing interval. In the surf zone, the cross shore mass flux is high and therefore a buoy can be translated quickly as a wave interacts with it. Therefore, if the location of the wave is inaccurate, the normalized wave height may be as well and could be skewed high due to quickly moving into shallower water. More validation and work on this aspect is needed in the future; however, the main takeaway is that in general the new instruments and processing methods are able to reproduce previous and expected measurements of the dynamics in the surf zone and therefore can be used with high confidence to further investigate the surf zone dynamics in a wave-resolving framework. In addition, the individual wave analysis suggests that wave-averaged metrics like γ may not be adequate to fully describe the wave transformation.

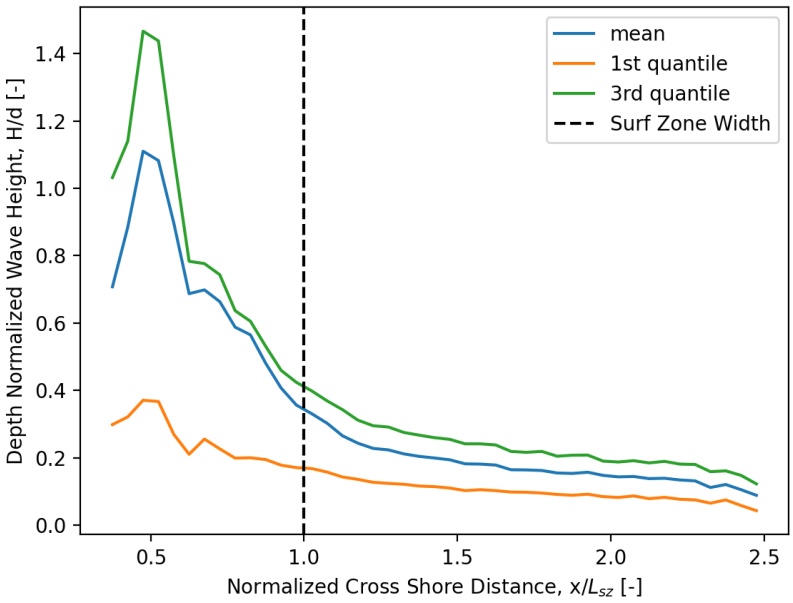

Figure 3.3: Mean, first and third quantile values of distributions of individual wave heights normalized by local water depth in cross shore distance bins normalized by an estimated surfzone width.

Chapter 4

DISCUSSION

The present study sits at the intersection between instrument development, data processing methodology, and the study of nearshore dynamics. We have created a small, low cost, and robust wave buoy that effectively measures the kinematics of the sea surface. From this new instrument, we created a large dataset that spans a wide range of wave forcing conditions. To make this happen, we have relied heavily on the many lessons learned over previous studies on how to design and handle data from wave buoys. While we have addressed some previous shortcomings on buoy development, such as motion correction and filtering to handle low frequency signal contamination, we have not gotten anything for free. Rather, by solving some challenges we have introduced new components that need to be examined with a healthy level of skepticism to effectively use this dataset. The components that we will need to watch closely in the future are the frequency limitations of the dataset, potential phase shifts and spikes introduced from motion correction along with the hydrodynamics of the microSWIFTs.

4.1 Frequency Limitations of Dataset

Numerical integration is known to lead to drift in signals due to accumulated error. These accumulated integration errors tend to manifest themselves as low frequency motion. While we would love to have an instrument that can measure all scales of motion, we are limited by this low frequency contamination in the integrated signals. To alleviate this contamination, we apply a digital band-pass filter at each integration step from acceleration to position. The filter is applied forward and backward which is known to have zero phase shifting [*Mitra and Kuo*, 2006]. As described in the methods section, the filter applied has frequency cut-offs

at 0.05 and 0.5 Hz. This was chosen to create the best surface gravity wave products and eliminate drift from integration while not interfering within the gravity wave frequency band. However, this limits our ability to study processes outside of this frequency range. Using these processing methods, we will not be able to investigate low frequency motions in the surf zone. While studying these low frequency motions, such as infra-gravity waves, is not the intended use of this data we want to be clear that this dataset is not applicable within this range for all measurements from the IMU. Measurements from the GPS have not been filtered in the same way and therefore there is potential to study lower frequency motions with these measurements in the future.

4.2 Phase Shifts and Data Spikes in Signals due to Motion Correction

As described in Chapter 2, the accelerations are corrected from the body reference frame to the earth reference frame through an indirect Kalman Filter sensor fusion algorithm. While this is the state-of-the-art for heading estimation, the highly nonlinear motions of the buoys, especially in and near breaking waves, may still cause spurious shifts and spikes in the data. To ensure no values were completely unreasonable prior to estimating the heading, each IMU data channel was despiked as described in the methods section previously using the PCHIP method. While we find this to be the most reasonable method of despiking, since it creates a continuous record, it is still an alteration to the original data and could still come with unforeseen consequences down the line. As we saw in Chapter 3, the microSWIFTs agrees well with other instrumentation in a statistical sense. However, due to the free-drifting nature of the microSWIFTs we have not directly validated these correction methods on a phase-resolving framework with fixed instrumentation. This will be left to future studies but it something to be cautious of moving forward. There could be potential small shifts or data spikes introduced to the data through the correction methods and while we expect these errors to be small, we have not fully quantified the extent of the potential errors.

4.3 Dynamics in the Motion of the microSWIFTs

On top of the challenges in processing the data from the microSWIFTs, we must also acknowledge the challenges we face with how the microSWIFTs act in the water and how we interpret their motion. The microSWIFTs don't exactly follow the waves, they don't exactly follow the currents, and they don't exactly follow the wind. Rather their trajectories are a complex combination of each of these components. The microSWIFTs are very buoyant and stay on the surface. We can then say with confidence that the microSWIFTs move up and down with the sea surface very well and therefore we have a high level of trust in the vertical wave motion measured from the microSWIFTs. While in the field, we saw that the microSWIFTs appeared to be affected by the wind and moved offshore when there was an offshore breeze. While at first this may seem to be an effect of the wind pushing directly on the microSWIFT, we believe it is due to the uppermost surface currents being strongly affected by the wind.

When the microSWIFT is in the water, the area above and below the surface is approximately equal. Since these areas are approximately equal, the drag force on the microSWIFT is primarily a balance between the density and velocity differences of the wind and currents. Due to the significantly higher density of the seawater compared to air we expect the microSWIFT to be primarily following the surface currents expect under extreme wind conditions. However, due to the shallow keel of the microSWIFT we expect the microSWIFT is really only following the top 4.5-5 cm of the surface currents. This uppermost layer on the surface is also heavily impacted by the wind which we believe is the reason that we observed the microSWIFTs moving offshore even during a modest offshore breeze.

Due to their small size and high buoyancy, the microSWIFTs also tend to "surf" on broken waves. This is again not solely following the surface currents in the surf zone. It most likely will not be possible to fully decouple this from actual surface currents since we will not be able to separate the times a microSWIFT is "surfing" a broken wave or just moving in a fast current. Therefore, we must treat the trajectory measurements as a combination

of all of these factors. In the future, we plan to use the trajectories of the microSWIFTs to investigate surf zone circulation. The measured trajectories of the microSWIFTs will not be able to tell us solely about the currents nor the waves or wind. However, the microSWIFT trajectories will be able to us about how realistic, highly buoyant particles move on the surface of the ocean in the inner shelf and surf zone as a combination of each of these components. Understanding how these types of particles move in the surf zone in realistic contexts can help us to understand how plastics, pollutants, and other tracers that are confined to the surface are transported in the real ocean.

Chapter 5

CONCLUSIONS

A unique dataset of measurements of surface gravity waves and surface currents in the inner shelf and surf zone was created through the use of large, coherent arrays of small-scale, free-drifting wave buoys named microSWIFTs. The coherent arrays provide high spatial and temporal resolution measurements for short bursts of time.

Wave buoys are omnipresent in the measurement of surface gravity waves in a range of environments; however, accurate measurements of shallow water waves in the inner shelf and surf zone have been challenging to obtain. Many wave buoys have been constrained to further offshore applications due to the data processing methods that include an implicit assumption of circular wave orbitals that makes them not applicable for surf zone measurements where waves are nonlinear and orbitals are elliptical. The processing of data from the microSWIFT wave buoys used in this experiment involves a correction of directly measured accelerations from the body frame of reference to the earth frame of reference through a 9-axis indirect Kalman filter used for attitude estimation. The correction is necessary to produce reliable measurements from the highly nonlinear and complex motion of the buoys as they transit the surf zone. The microSWIFTs produce estimates of significant wave heights that have strong, statistically significant, agreement with previously verified fixed instrumentation. The microSWIFT arrays can also accurately reproduce previous results of wave height transformation across the inner shelf and surf zone and therefore can be used with high confidence to further explore the inner shelf and surf zone dynamics.

Many field experiments in the past have investigated how bulk parameters and wave spectra evolve in the inner shelf and surf zone. Moving forward, we plan to use this dataset to investigate the surf zone in a wave-resolving framework. Using a breaking identifier algorithm

developed in [*Brown et al.*, 2018] we can detect when a microSWIFT is in a breaking wave which can then be used to locate individual breaking waves. This identifier can also be used as a proxy for the strength of the breaker which can be used to investigate energetics in the surf zone. Using these methods in conjunction with bathymetry measurements and imagery at the field site we hope to test the applicability of different breaking onset and strength parameterizations over a large range of conditions. In particular, we plan to use this dataset to further investigate the breaking onset and strength parameterizations postulated by [*Barthelemy et al.*, 2018]. We also plan to investigate the applicability of the assumption of an energy saturated surf zone over various conditions. We will explore the circulation patterns in the surf zone and inner shelf through the microSWIFT array drift tracks. The microSWIFTs follow the surface of the ocean well; however, they are affected by the wind and they also tend to "surf" on the broken waves. With this in mind, we will look at the transport and circulation of buoyant particles in the surf zone under different wave conditions. The unique ability of this dataset to investigate phase-resolved wave processes will be used to find a connection between the intermittent process of wave breaking and phase-averaged, operational wave models.

BIBLIOGRAPHY

Abel, J. R., J. Bram, R. Deitz, J. A. Orr, et al., What are the costs of superstorm sandy?, *Tech. rep.*, Federal Reserve Bank of New York, 2012.

Barthelemy, X., M. Banner, W. Peirson, F. Fedele, M. Allis, and F. Dias, On a unified breaking onset threshold for gravity waves in deep and intermediate depth water, *Journal of Fluid Mechanics*, *841*, 463–488, 2018.

Basco, D. R., and M. Asce, A Qualitative Description of Wave Breaking, p. 18, 1985.

Battjes, J. A., Surf-Zone Dynamics, *Annual Review of Fluid Mechanics*, *20*(1), 257–291, doi:10.1146/annurev.fl.20.010188.001353, _eprint: https://doi.org/10.1146/annurev.fl.20.010188.001353, 1988.

Battjes, J. A., and J. P. F. M. Janssen, ENERGY LOSS AND SET-UP DUE TO BREAKING OF RANDOM WAVES, *Coastal Engineering Proceedings*, (16), 32–32, doi: 10.9753/icce.v16.32, number: 16, 1978.

Bertin, X., Storm surges and coastal flooding: status and challenges, *La Houille Blanche*, *102*(2), 64–70, doi:10.1051/lhb/2016020, 2016.

Boehm, A. B., N. S. Ismail, L. M. Sassoubre, and E. A. Andruszkiewicz, Oceans in Peril: Grand Challenges in Applied Water Quality Research for the 21st Century, *Environmental Engineering Science*, *34*(1), 3–15, doi:10.1089/ees.2015.0252, publisher: Mary Ann Liebert, Inc., publishers, 2017.

Brown, A., J. Thomson, A. Ellenson, F. T. Rollano, H. T. Özkan-Haller, and M. C. Haller, Kinematics and statistics of breaking waves observed using swift buoys, *IEEE Journal of Oceanic Engineering*, *44*(4), 1011–1023, 2018.

Butt, T., P. Russell, J. Puleo, J. Miles, and G. Masselink, The influence of bore turbulence on sediment transport in the swash and inner surf zones, *Continental Shelf Research*, *24*(7-8), 757–771, doi:10.1016/j.csr.2004.02.002, 2004.

Carini, R. J., C. C. Chickadel, A. T. Jessup, and J. Thomson, Estimating wave energy dissipation in the surf zone using thermal infrared imagery, *Journal of Geophysical Research: Oceans*, *120*(6), 3937–3957, doi:10.1002/2014JC010561, _eprint: https://onlinelibrary.wiley.com/doi/pdf/10.1002/2014JC010561, 2015.

Cavaleri, L., Wave modeling—missing the peaks, *Journal of Physical Oceanography*, *39*(11), 2757–2778, 2009.

Collins, C. O., B. Lund, T. Waseda, and H. C. Graber, On recording sea surface elevation with accelerometer buoys: lessons from ITOP (2010), *Ocean Dynamics*, *64*(6), 895–904, doi:10.1007/s10236-014-0732-7, 2014.

Derakhti, M., J. T. Kirby, M. L. Banner, S. T. Grilli, and J. Thomson, A Unified Breaking Onset Criterion for Surface Gravity Water Waves in Arbitrary Depth, *Journal of Geophysical Research: Oceans*, *125*(7), e2019JC015,886, doi:10.1029/2019JC015886, _eprint: https://onlinelibrary.wiley.com/doi/pdf/10.1029/2019JC015886, 2020.

Dysthe, K., H. Krogstad, and P. Müller, Rogue Waves, *Encyclopedia of Ocean Sciences*, pp. 770–780, doi:10.1016/B978-012374473-9.00612-3, 2010.

Feddersen, F., R. T. Guza, S. Elgar, and T. H. C. Herbers, Alongshore momentum balances in the nearshore, *Journal of Geophysical Research: Oceans*, *103*(C8), 15,667–15,676, doi:10.1029/98JC01270, 1998.

Feddersen, F., J. H. Trowbridge, and A. J. Williams, Vertical Structure of Dissipation in the Nearshore, *Journal of Physical Oceanography*, *37*(7), 1764–1777, doi:10.1175/JPO3098.1, 2007.

Galvin, C. J., Wave breaking in shallow water, *Waves on beaches and resulting sediment transport*, pp. 413–456, 1972.

Grasso, F., and B. G. Ruessink, Vertical structure of the turbulence dissipation rate in the surf zone, *Journal of Coastal Research*, pp. 90–94, publisher: Coastal Education & Research Foundation, Inc., 2011.

Herbers, T. H. C., N. R. Russnogle, and S. Elgar, Spectral Energy Balance of Breaking Waves within the Surf Zone, *Journal of Physical Oceanography*, *30*(11), 2723–2737, doi:10.1175/1520-0485(2000)030⟨2723:SEBOBW⟩2.0.CO;2, publisher: American Meteorological Society Section: Journal of Physical Oceanography, 2000.

Herbers, T. H. C., P. F. Jessen, T. T. Janssen, D. B. Colbert, and J. H. MacMahan, Observing Ocean Surface Waves with GPS-Tracked Buoys, *Journal of Atmospheric and Oceanic Technology*, *29*(7), 944–959, doi:10.1175/JTECH-D-11-00128.1, publisher: American Meteorological Society Section: Journal of Atmospheric and Oceanic Technology, 2012.

Jackson, D., and A. Short, *Sandy beach morphodynamics*, Elsevier, 2020.

Johnson, D., and C. Pattiaratchi, Transient rip currents and nearshore circulation on a swell-dominated beach, *Journal of Geophysical Research: Oceans*, *109*(C2), 2004.

Kalman, R. E., A new approach to linear filtering and prediction problems, 1960.

Kuik, A. J., G. P. v. Vledder, and L. H. Holthuijsen, A Method for the Routine Analysis of Pitch-and-Roll Buoy Wave Data, *Journal of Physical Oceanography*, *18*(7), 1020–1034, doi:10.1175/1520-0485(1988)018⟨1020:AMFTRA⟩2.0.CO;2, publisher: American Meteorological Society Section: Journal of Physical Oceanography, 1988.

Labbe, R., Kalman and bayesian filters in python, *Chap*, *7*(246), 4, 2014.

Lenau, C. W., The solitary wave of maximum amplitude, *Journal of Fluid Mechanics*, *26*(2), 309–320, doi:10.1017/S0022112066001253, 1966.

Lentz, S. J., and M. R. Fewings, The wind-and wave-driven inner-shelf circulation, *Annual review of marine science*, *4*, 317–343, 2012.

Longuet-Higgins, M. S., On the distribution of the heights of sea waves: Some effects of nonlinearity and finite band width, *Journal of Geophysical Research: Oceans*, *85*(C3), 1519–1523, 1980.

Longuet-Higgins, M. S., and R. Stewart, Radiation stresses in water waves; a physical discussion, with applications, in *Deep sea research and oceanographic abstracts*, vol. 11, pp. 529–562, Elsevier, 1964.

MacMahan, J. H., E. B. Thornton, and A. J. H. M. Reniers, Rip current review, *Coastal Engineering*, *53*(2), 191–208, doi:10.1016/j.coastaleng.2005.10.009, 2006.

McCowan, J., Xxxix. on the highest wave of permanent type, *The London, Edinburgh, and Dublin Philosophical Magazine and Journal of Science*, *38*(233), 351–358, 1894.

Melville, W. K., The role of surface-wave breaking in air-sea interaction, 1996.

Michener, W. K., E. R. Blood, K. L. Bildstein, M. M. Brinson, and L. R. Gardner, Climate change, hurricanes and tropical storms, and rising sea level in coastal wetlands, *Ecological Applications*, *7*(3), 770–801, 1997.

Mitra, S. K., and Y. Kuo, *Digital signal processing: a computer-based approach*, vol. 2, McGraw-Hill New York, 2006.

Moulton, M., S. Elgar, B. Raubenheimer, J. C. Warner, and N. Kumar, Rip currents and alongshore flows in single channels dredged in the surf zone, *Journal of Geophysical Research: Oceans*, *122*(5), 3799–3816, doi:10.1002/2016JC012222, _eprint: https://agupubs.onlinelibrary.wiley.com/doi/pdf/10.1002/2016JC012222, 2017.

Neumann, J. E., K. Emanuel, S. Ravela, L. Ludwig, P. Kirshen, K. Bosma, and J. Martinich, Joint effects of storm surge and sea-level rise on us coasts: new economic estimates of

impacts, adaptation, and benefits of mitigation policy, *Climatic Change*, *129*(1), 337–349, 2015.

Perlin, M., W. Choi, and Z. Tian, Breaking waves in deep and intermediate waters, *Annual review of fluid mechanics*, *45*, 115–145, 2013.

PINEDA, J., J. A. HARE, and S. SPONAUGLE, Larval Transport and Dispersal in the Coastal Ocean and Consequences for Population Connectivity, *Oceanography*, *20*(3), 22–39, publisher: Oceanography Society, 2007.

Raghukumar, K., G. Chang, F. Spada, C. Jones, T. Janssen, and A. Gans, Performance Characteristics of "Spotter," a Newly Developed Real-Time Wave Measurement Buoy, *Journal of Atmospheric and Oceanic Technology*, *36*(6), 1127–1141, doi:10.1175/JTECH-D-18-0151.1, publisher: American Meteorological Society Section: Journal of Atmospheric and Oceanic Technology, 2019.

Raubenheimer, B., R. T. Guza, and S. Elgar, Wave transformation across the inner surf zone, *Journal of Geophysical Research: Oceans*, *101*(C11), 25,589–25,597, doi:10.1029/96JC02433, _eprint: https://onlinelibrary.wiley.com/doi/pdf/10.1029/96JC02433, 1996.

Roetenberg, D., H. Luinge, C. Baten, and P. Veltink, Compensation of magnetic disturbances improves inertial and magnetic sensing of human body segment orientation, *IEEE Transactions on Neural Systems and Rehabilitation Engineering*, *13*(3), 395–405, doi:10.1109/TNSRE.2005.847353, conference Name: IEEE Transactions on Neural Systems and Rehabilitation Engineering, 2005.

Rogers, W. E., J. Thomson, H. H. Shen, M. J. Doble, P. Wadhams, and S. Cheng, Dissipation of wind waves by pancake and frazil ice in the autumn b eaufort s ea, *Journal of Geophysical Research: Oceans*, *121*(11), 7991–8007, 2016.

Sabatini, A. M., Kalman-Filter-Based Orientation Determination Using Inertial/Magnetic

Sensors: Observability Analysis and Performance Evaluation, *Sensors*, *11*(10), 9182–9206, doi:10.3390/s111009182, 2011.

Saket, A., W. L. Peirson, M. L. Banner, X. Barthelemy, and M. J. Allis, On the threshold for wave breaking of two-dimensional deep water wave groups in the absence and presence of wind, *Journal of Fluid Mechanics*, *811*, 642–658, 2017.

Schmidt, W. E., B. T. Woodward, K. S. Millikan, R. T. Guza, B. Raubenheimer, and S. Elgar, A GPS-Tracked Surf Zone Drifter, *Journal of Atmospheric and Oceanic Technology*, *20*(7), 1069–1075, doi:10.1175/1460.1, publisher: American Meteorological Society Section: Journal of Atmospheric and Oceanic Technology, 2003.

Schmidt, W. E., R. T. Guza, and D. N. Slinn, Surf zone currents over irregular bathymetry: Drifter observations and numerical simulations, *Journal of Geophysical Research*, *110*(C12), C12,015, doi:10.1029/2004JC002421, 2005.

Smith, M., and J. Thomson, Ocean surface turbulence in newly formed marginal ice zones, *Journal of Geophysical Research: Oceans*, *124*(3), 1382–1398, 2019.

Spydell, M., F. Feddersen, R. T. Guza, and W. E. Schmidt, Observing Surf-Zone Dispersion with Drifters, *Journal of Physical Oceanography*, *37*(12), 2920–2939, doi:10.1175/2007JPO3580.1, publisher: American Meteorological Society Section: Journal of Physical Oceanography, 2007.

Thomson, J., Wave Breaking Dissipation Observed with "SWIFT" Drifters, *Journal of Atmospheric and Oceanic Technology*, *29*(12), 1866–1882, doi:10.1175/JTECH-D-12-00018.1, publisher: American Meteorological Society Section: Journal of Atmospheric and Oceanic Technology, 2012.

Thomson, J., and W. E. Rogers, Swell and sea in the emerging arctic ocean, *Geophysical Research Letters*, *41*(9), 3136–3140, 2014.

Thomson, J., M. S. Schwendeman, S. F. Zippel, S. Moghimi, J. Gemmrich, and W. E. Rogers, Wave-breaking turbulence in the ocean surface layer, *Journal of Physical Oceanography*, *46*(6), 1857–1870, 2016.

Thomson, J., J. B. Girton, R. Jha, and A. Trapani, Measurements of Directional Wave Spectra and Wind Stress from a Wave Glider Autonomous Surface Vehicle, *Journal of Atmospheric and Oceanic Technology*, *35*(2), 347–363, doi:10.1175/JTECH-D-17-0091.1, publisher: American Meteorological Society Section: Journal of Atmospheric and Oceanic Technology, 2018.

Thornton, E. B., and R. T. Guza, Energy saturation and phase speeds measured on a natural beach, *Journal of Geophysical Research: Oceans*, *87*(C12), 9499–9508, doi:10.1029/JC087iC12p09499, _eprint: https://onlinelibrary.wiley.com/doi/pdf/10.1029/JC087iC12p09499, 1982.

Thornton, E. B., and R. T. Guza, Transformation of wave height distribution, *Journal of Geophysical Research: Oceans*, *88*(C10), 5925–5938, doi:10.1029/JC088iC10p05925, _eprint: https://onlinelibrary.wiley.com/doi/pdf/10.1029/JC088iC10p05925, 1983.

Ursell, F., Wave generation by wind, *Surveys in mechanics*, pp. 216–249, 1956.

Vitousek, P. M., H. A. Mooney, J. Lubchenco, and J. M. Melillo, Human Domination of Earth's Ecosystems, *277*, 7, 1997.

Appendix A

MISSION DESCRIPTIONS

Mission Number	Date	Duration [minutes]	Number of Buoys	Deployment Method
1	10/4/21	17	12	surfboard
2	10/5/21	8	6	surfboard
3	10/5/21	20	9	surfboard
4	10/5/21	11	9	surfboard
5	10/5/21	10	9	surfboard
6	10/4/21	5	5	surfboard
7	10/6/21	170	8	helicopter
8	10/7/21	14	9	pier
9	10/7/21	10	9	jetski
10	10/7/21	24	8	jetski
11	10/7/21	9	9	jetski
12	10/7/21	16	17	jetski
13	10/7/21	21	18	pier
14	10/7/21	14	18	jetski
15	10/8/21	21	34	pier
16	10/8/21	22	32	jetski
17	10/8/21	17	32	jetski
18	10/8/21	38	32	jetski
19	10/8/21	28	32	jetski
20	10/10/21	11	51	pier
21	10/10/21	18	51	pier

Mission Number	Date	Duration [minutes]	Number of Buoys	Deployment Method
22	10/10/21	8	47	pier
23	10/10/21	10	47	pier
24	10/11/21	17	39	pier
25	10/11/21	22	39	pier
26	10/11/21	28	38	pier
27	10/11/21	45	37	pier
28	10/12/21	23	22	jetski
29	10/13/21	20	10	jetski
30	10/13/21	35	19	jetski
31	10/13/21	21	20	jetski
32	10/13/21	11	29	jetski
33	10/14/21	19	10	jetski
34	10/14/21	15	10	jetski
35	10/14/21	20	15	jetski
36	10/14/21	17	13	jetski
37	10/14/21	7	16	jetski
38	10/14/21	32	30	jetski
39	10/15/21	15	16	surfboard
40	10/15/21	36	16	surfboard
41	10/17/21	7	15	jetski
42	10/17/21	23	24	jetski and drone
43	10/17/21	8	27	jetski and drone
44	10/18/21	39	20	pier
45	10/18/21	14	20	pier
46	10/19/21	3	12	jetski
47	10/19/21	5	12	jetski

Mission Number	Date	Duration [minutes]	Number of Buoys	Deployment Method
48	10/19/21	10	12	jetski
49	10/19/21	10	12	jetski
50	10/19/21	21	23	jetski
51	10/22/21	50	2	surfboard
52	10/22/21	60	2	surfboard
53	10/23/21	22	4	surfboard
54	10/25/21	26	16	surfboard
55	10/25/21	37	16	surfboard
56	10/25/21	33	16	surfboard
57	10/26/21	12	10	jetski
58	10/26/21	9	10	jetski
59	10/26/21	23	10	jetski
60	10/27/21	16	8	helicopter
61	10/27/21	1	8	jetski
62	10/27/21	3	30	pier
63	10/27/21	25	38	pier
64	10/27/21	14	38	pier
65	10/27/21	24	38	pier
66	10/28/21	11	27	pier
67	10/28/21	16	27	pier
68	10/28/21	16	34	helicopter and pier
69	10/28/21	13	34	pier
70	10/28/21	4	34	pier
71	10/28/21	13	33	pier
72	10/28/21	22	33	pier
73	10/28/21	10	31	pier

Mission Number	Date	Duration [minutes]	Number of Buoys	Deployment Method
74	10/29/21	10	31	pier
75	10/29/21	6	31	pier
76	10/29/21	8	31	pier
77	10/29/21	6	39	pier
78	10/29/21	11	39	pier
79	10/29/21	7	39	pier
80	10/29/21	6	39	pier
81	10/29/21	13	39	pier

Table A.1: Description of each deployment of a coherent array or "mission" during the DUNEX experiment.

Appendix B

DATA CLEANING NOTES

All adjustments to each individual mission are adjustments made to the originally written down start and end times which were written approximately while in the field. All values that are masked refer to values begin filled with NaN values.

Mission 1 (Cleaned on 02/24/22):

- Adjusted the end time from 2021-10-04T15:30:00 to 2021-10-04T15:17:00 since the microSWIFTs started being picked up at this point

Mission 2(Cleaned on 02/24/22):

- Adjusted start time from 2021-10-05T14:30:00 to 2021-10-05T14:41:00 since the microSWIFTs were still on surfboards until this point.
- Adjusted end time from 2021-10-05T16:00:00 to 2021-10-05T14:50:00 since all of the microSWIFTs have reached the beach at this point.
- Masked microSWIFT 4 from the start to index 200 since it was still on a surfboard as seen by smaller signals then a large spike in acceleration as it is thrown in
- Masked microSWIFT 5 from the start to index 200 since it was still on a surfboard as seen by smaller signals then a large spike in acceleration as it is thrown in
- Masked microSWIFT 3 from the start to index 200 since it was still on a surfboard as seen by smaller signals then a large spike in acceleration as it is thrown in

Mission 3(Cleaned on 02/24/22):

- Adjusted start time from 2021-10-05T17:10:00 to 2021-10-05T17:17:00 since the microSWIFTs were still on the surfboards at this point as seen by fast offshore movement.

- Adjusted end time from 2021-10-05T17:40:00 to 2021-10-05T17:37:00 since all of the microSWIFTs had reached the beach at this point.

- Masked microSWIFT 40 from index 7000 to the end since it reached the beach and a few points were not masked as it maybe moved back offshore briefly after passing the spatial threshold

- Masked microSWIFT 3 from index 9000 to the end since it reached the beach and a few points were not masked as it maybe moved back offshore briefly after passing the spatial threshold

- Masked microSWIFT 39 from index 4500 to the end since it reached the beach and a few points were not masked as it maybe moved back offshore briefly after passing the spatial threshold

- Masked microSWIFT 41 from index 8500 to the end since it reached the beach and a few points were not masked as it maybe moved back offshore briefly after passing the spatial threshold

Mission 4(Cleaned on 02/25/22):

- Adjusted start time from 2021-10-05T18:06:00 to 2021-10-05T18:13:00 since the microSWIFTs were still on the surfboards as seen by them moving quickly offshore before deployment

- Adjusted end time from 2021-10-05T18:35:00 to 2021-10-05T18:24:00 since all of the microSWIFTs had based the beach spatial mask at this point.

- Masked microSWIFT 40 from index 6800 to the end since it passed the spatial threshold but moved back out briefly.

- Masked microSWIFT 40 from index 6500 to the end since it passed the spatial threshold but moved back out briefly.

- Masked microSWIFT 40 from index 7000 to the end since it passed the spatial threshold but moved back out briefly.

Mission 5(Cleaned on 03/01/22):

- Adjusted the start time from 2021-10-05T18:35:00 to 2021-10-05T18:40:00 since the microSWIFTs were still on the surfboard at this point

- Masked microSWIFT 3 from the start to index 1500 since the IMU was not recording correctly at this point as seen by a non fluctuating acceleration signal

- Masked microSWIFT 42 from the start to index 500 since it had a large spike in acceleration most likely due to being thrown

- Masked microSWIFT 39 from the start to index 500 since it had a large spike in acceleration most likely due to being thrown

- Masked microSWIFT 5 from the start to index 1000 since it had a large spike in acceleration most likely due to being thrown into the water

- Masked microSWIFT 38 from the start to index 1500 since the IMU was not recording correctly at this point as seen by a non fluctuating acceleration signal

- Removed microSWIFT 40 since it had unreasonably high sea surface elevations (5 meters) most likely due to a short record(2500 points)

- Removed microSWIFT 41 since it had unreasonably high sea surface elevations (5 meters) most likely due to a short record(2500 points)

- Removed microSWIFT 57 since it had a huge spike in acceleration and value of sea surface elevation of 300 meters due to potentially a malfunction in the accelerometer or gyroscope

Mission 6(Cleaned on 02/25/22):

- Not a separate mission from mission 1 but these are the microSWIFTs that drifted super far north - removed from the cleaned dataset since it is not useful data for this project - all buoys are far from test site and in deep/intermediate water

Mission 7(Cleaned on 02/25/22):

- Masked microSWIFT 40 from index 36000 to the end since it reached the beach in the send window so we are masking from the start of the send window to the end

- Masked microSWIFT 40 from index 36000 to the end since it reached the beach in the send window so we are masking from the start of the send window to the end

- Masked microSWIFT 40 from index 36000 to the end since it reached the beach in the send window so we are masking from the start of the send window to the end

Mission 8(Cleaned on 02/25/22):

- Adjusted start time from 2021-10-07T14:00:00 to 2021-10-07T14:02:00 since a few of the microSWIFTs were still on the pier at this point as seen by flat acceleration signals

- Adjusted end time from 2021-10-07T14:20:00 to 2021-10-07T14:16:00 since all of the microSWIFTs had reached the beach at this point.

Mission 9(Cleaned on 02/25/22):

- Only two microSWIFTs went out - this is a small mission - not sure why the location of one of the microSWIFTs cuts out before the beach, must have lost GPS signal

- Adjusted the end time from 2021-10-07T14:50:00 to 2021-10-07T14:40:00 since both microSWIFTs had reached the beach at this point

Mission 10(Cleaned on 01/26/22):

- Moved start time from 2021-10-07T14:40:00 to 2021-10-07T14:46:15 since the microSWIFTs were still on the jetski until then as seen from visual inspection from plotting with the original dataset.

Mission 11(Cleaned on 01/26/22):

- Adjusted start time from 2021-10-07T15:10:00 to 2021-10-07T15:12:00 since the microSWIFTs are still moving offshore on the jetski prior to deployment.

- Adjusted end time from 2021-10-07T16:00:00 to 2021-10-07T15:21:00 since almost every microSWIFT hit the beach before this except for microSWIFT 34.

- Deleted microSWIFT 41 from dataset since it is missing almost all GPS data and therefore we can't use it.

- microSWIFT 34 was still on the jetski and was not deployed until about 2.7 minutes (index 2000) after the other so it is individually being masked from the beginning

Mission 12(Cleaned on 01/26/22):

- Adjusted start time from 2021-10-07T16:00:00 to 2021-10-07T16:05:30 since the microSWIFTs do not have a wave signal until this index (mostly flat signal)

- Adjusted end time from 2021-10-07T16:30:00 to 2021-10-07T16:21:00 since all microSWIFTs have reached the beach by this point.

- microSWIFT 57 has one spot at the end of the time series that isn't getting masked after index 10000 so we will manually mask it

Mission 13(Cleaned on 01/26/22):

- Adjusted start time from 2021-10-07T17:00:00 to 2021-10-07T17:02:45 since the microSWIFTs were all still stationary on the pier until this time.

- Adjusted end time from 2021-10-07T17:25:00 to 2021-10-07T17:23:00 since all of the microSWIFTs had reached the beach before this point.

Mission 14(Cleaned on 01/26/22):

- Adjusted start time from 2021-10-07T18:00:00 to 2021-10-07T18:01:00 since the first few data points of a couple show a signal that is not quite in the water since it is a mostly flat signal.

- Adjusted end time from 2021-10-07T18:35:00 to 2021-10-07T18:15:30 since almost every microSWIFT reached the beach before this time and the few that did not were caught in a swash zone eddy so the data is not useful for this project.

- Note that microSWIFT 38's magnetometer was not working so it recorded all zeros in all directions

Mission 15(Cleaned on 01/26/22):

- Adjusted end time from 2021-10-08T13:46:00 to 2021-10-08T13:38:00 since almost all microSWIFTs reached the beach before that time.

Mission 16(Cleaned on 01/26/22):

- Adjusted the start time from 2021-10-08T14:05:00 to 2021-10-08T14:10:30 since most the microSWIFTs were not in the water at this point as seen by a mostly flat signal in all IMU measurements.

- Adjusted the end time from 2021-10-08T14:46:00 to 2021-10-08T14:32:00 since all of the microSWIFTs had made it to the beach at this point.

- Removed microSWIFT 41 since it has only a very small amount of data mostly before any of the others were deployed (<1000 points)

- Removed microSWIFT 37 since it has only a very small amount of data mostly before any of the others were deployed (<1000 points)

- Removed microSWIFT 44 since it has only a very small amount of data mostly before any of the others were deployed (<1000 points)

- Removed microSWIFT 43 since it has only a very small amount of data mostly before any of the others were deployed (<1000 points)

- Removed microSWIFT 16 since it has only a very small amount of data mostly before any of the others were deployed (<1000 points)

- Removed microSWIFT 42 since it has only a very small amount of data mostly before any of the others were deployed (<1000 points)

- Removed microSWIFT 34 since it has only a very small amount of data mostly before any of the others were deployed (<1000 points)

- Removed microSWIFT 33 since it has only a very small amount of data mostly before any of the others were deployed (<1000 points)

Mission 17(Cleaned on 01/26/22):

- Adjusted start time from 2021-10-08T15:00:00 to 2021-10-08T15:04:30 since most of the microSWIFTs are still on the jetski at this point as we can see be a non-wave looking IMU signal.

- Adjusted end time from 2021-10-08T16:00:00 to 2021-10-08T15:25:00 since most of the microSWIFTs reached the beach by this point.

- Removed microSWIFT 46 since it is missing all xFRF values meaning it did not have good GPS data.

- Removed microSWIFTs 13, 22, 41, 12, 21, 11, 42, 34 and 33 since they were all deployed before the further offshore one and made it to the beach before each other microSWIFT was deployed.

- microSWIFT 44 is masked from index 9000 to the end since it has not real looking signals from the IMU which indicates it is most likely on the beach.

Mission 18(Cleaned on 01/26/22):

- Adjusted start time from 2021-10-08T17:00:00 to 2021-10-08T17:04:30 since most of the microSWIFTs were still on the jetski at this point in time.

- Adjusted end time from 2021-10-08T18:00:00 to 2021-10-08T17:42:00 since all of the microSWIFTs have reached the beach at this point.

- microSWIFT 12 is masked from index 20000 to the end since it has reached the beach and potentially rolled back down briefly.

Mission 20(Cleaned on 01/26/22):

- Adjusted end time from 2021-10-10T13:27:00 to 2021-10-10T13:18:15 since almost all microSWIFTs had made it to the beach at that point.

- Removed microSWIFT 58 since it has a bad gyroscope

- Removed microSWIFT 31 since it has a bad gyroscope

- microSWIFT 26 must have rolled back down the beach past the spatial cutoff and needs to be masked from index 7000 to the end.

Mission 21(Cleaned on 01/26/22):

- Adjusted end time from 2021-10-10T14:36:00 to 2021-10-10T14:25:00
- Removed microSWIFT 58 since it has a bad gyroscope
- microSWIFT 7 is masked from index 10,000 to the end since there is weird looking IMU data after this index
- microSWIFT 26 is masked from index 7000 to the end since the microSWIFT looks like it rolls back down the beach past the spatial cutoff.

Mission 22(Cleaned on 01/26/22):

- Adjusted end time from 2021-10-10T15:27:00 to 2021-10-10T15:15:30 since all the microSWIFTs reached the beach before this point.
- Removed microSWIFT 58 since it has a bad gyroscope
- Removed microSWIFT 31 since it has a bad magnetometer due to mostly flat readings
- microSWIFT 13 looks like it made it to the beach with flat IMU signals but is not masked by the spatial mask.

Mission 23(Cleaned on 01/26/22):

- Adjusted start time from 2021-10-10T16:05:30 to 2021-10-10T16:11:00 since most of the microSWIFTs haven't been deployed by this point which can be seen by the flay IMU signals.

- Adjusted end time from 2021-10-10T16:35:00 to 2021-10-10T16:21:00 since all of the microSWIFTs have reached the beach by this point.

- Removed microSWIFT 58 since it has a bad gyro

- Removed microSWIFT 16 since it was missing GPS data

Mission 24(Cleaned on 01/26/22):

- Adjusted start time from 2021-10-11T13:05:00 to 2021-10-11T13:13:00 since most microSWIFTs haven't been deployed yet and we can see it in the flat signal.

- Adjusted end time from 2021-10-11T13:47:00 to 2021-10-11T13:30:00 since the microSWIFTs have all made it to the beach before this.

- Removed microSWIFT 12 since the IMU was not working and all signals were flat

- Removed microSWIFT 31 since it was missing a bunch of GPS data

Mission 25(Cleaned on 01/26/22):

- Adjusted start time from 2021-10-11T14:10:00 to 2021-10-11T14:11:00 since many of the microSWIFTs hadn't been deployed yet as seen by flat signals from the IMU.

- Adjusted end time from 2021-10-11T14:50:00 to 2021-10-11T14:33:00 since almost all the microSWIFTs made it to the beach before this time so it the time that the array is most coherent.

- Removed microSWIFT 58 since it has a bad gyro

- microSWIFT 31 is not getting masked for being on the beach which we can see in the flat IMU signals so we will manually mask from index 15000 to the end.

Mission 26(Cleaned on 01/27/22):

- Adjusted end time from 2021-10-11T17:00:00 to 2021-10-11T16:33:00
- magnetometer on microSWIFT 35 not working as seen by flat signals
- Removed microSWIFT 58 since it has a bad gyro

Mission 27(Cleaned on 01/28/22):

- Mask microSWIFT 27 from the start to index 100 since it looks like just a bit of the drop is included right at the beginning.
- Mask microSWIFTs 28, 56, 4, 34 and 50 from index 20000 to the end since it looks like they all made it to the beach and briefly rolled back down
- Removed microSWIFT 16 since it was missing a bunch of GPS data
- Removed microSWIFT 58 since it has a bad gyro
- Note that microSWIFT 56 has a bad magnetometer

Mission 28(Cleaned on 01/28/22):

- Adjusted start time from 2021-10-12T13:10:00 to 2021-10-12T13:22:00 since it looks like many of the microSWIFTs were still on the jetski before deployment at this point
- Adjusted end time from 2021-10-12T18:00:00 to 2021-10-12T13:45:00 since most microSWIFTs that stayed within the domain made it to the beach in this time while many other microSWIFTs went far out of the domain where we can't use the data so it is cut off here.
- Mask microSWIFT 24 from start to index 4000

- Removed microSWIFT 17 since it is missing GPS data
- Removed microSWIFT 58 since it is missing GPS data
- Removed microSWIFT 13, 24 and 57 from dataset since they hit the beach before anything else was deployed and had almost no data.

Mission 29(Cleaned on 01/28/22):

- Adjusted start time from 2021-10-13T13:00:00 to 2021-10-13T13:10:00 since all of the microSWIFTs were still on the jetski at this point which can be seen by the location and non-wave like IMU signals.
- Adjusted end time from 2021-10-13T13:35:00 to 2021-10-13T13:30:00 since all of the microSWIFTs made it to the beach by this point as seen by the signals being cutoff by the spatial mask.

Mission 30(Cleaned on 01/28/22):

- Adjusted start time from 2021-10-13T14:04:00 to 2021-10-13T14:18:00 since all of the microSWIFTs were still on the jetski at this point which can be seen by the movement towards the north side from the pier and non wave like signals in the IMU.
- Adjusted end time from 2021-10-13T15:15:00 to 2021-10-13T14:53:00 since all of the microSWIFTs made it the beach in this time as seen by the signals being cut off by the spatial mask.
- Removed microSWIFT 13 since it has bad gyroscope measurements(no fluctuations)
- Note that microSWIFT 3 has a bad magnetometer(no fluctuations in measurements)
- Mask microSWIFT 42 from index 15000 to the end since it made it to the beach but then rolled back down briefly.

Mission 31(Cleaned on 01/28/22):

- Adjusted start time from 2021-10-13T16:15:00 to 2021-10-13T16:22:00since most of the microSWIFTs are still on the jetski as seen by the irregular/ choppy GPS locations and non-wave like IMU signals.

- Adjust end time from 2021-10-13T17:00:00 to 2021-10-13T16:43:00 since almost all of the microSWIFTs made it to the beach by this time based on the spatial mask.

- Removed microSWIFTs 41, 2, 31 and 43 since all had already hit the beach by the time the others were deployed.

- Masking microSWIFTs 34, 33 and 35 from the start to index 1000 since they were still on the jetski being deployed during these indices.

- Mask microSWIFT 46 from start to index 2500 since it is still on the jetski at this point as seen by the choppy/irregular position signals.

Mission 32(Cleaned on 02/15/22):

- Adjusted end time from 2021-10-13T17:40:00 to 2021-10-13T17:31:00 since most of the microSWIFTs had reached the beach by this point.

- Removed microSWIFT 20 since it is missing GPS data

- Removed microSWIFT 18 since it is missing GPS data

- Removed microSWIFT 12 since it had only 500 data points

- Removed microSWIFT 27 since it had only 500 data points

- Masked microSWIFT 59 from the start to index 500 since it was missing data just after this section for 1000 points then the rest of the record has data

- Removed microSWIFTs 46, 2, 19, 29(almost no data 500 points), 56 and 58 since it is missing all data

Mission 33(Cleaned on 01/28/22):

- Adjusted start time from 2021-10-14T12:00:00 to 2021-10-14T12:21:00 since the microSWIFTs are still on the jetski up to this point.

- Adjusted end time from 2021-10-14T12:45:00 to 2021-10-14T12:40:30 since almost all of the microSWIFTs made it to the beach by this point.

- Mask microSWIFTs 43 and 35 from index 13000 to end since it looks like they were picked up by a jetski at this point.

Mission 34(Cleaned on 02/15/22):

- Adjusted start time from 2021-10-14T12:56:00 to 2021-10-14T13:00:00 to investigate problems with missing data.

- Removed microSWIFT 2 since it is missing GPS data

- Removed microSWIFT 36 since it is missing GPS data

- Removed microSWIFT 31 since it is missing GPS data

- Removed microSWIFT 43 since it is missing GPS data

- Removed microSWIFT 44 since it has less that 500 data points during the mission

- Removed microSWIFT 34 since it has less that 500 data points during the mission

- Removed microSWIFT 33 since it has less that 500 data points during the mission

- Removed microSWIFT 35 since it has less that 500 data points during the mission

Mission 35(Cleaned on 02/15/22):

- Adjusted start time from 2021-10-14T13:15:00 to 2021-10-14T13:23:00 since most the microSWIFTs were still on the jetski
- Adjusted end time from 2021-10-14T14:00:00 to 2021-10-14T13:43:30 since most of the microSWIFTs made it to the beach at this point
- Removed microSWIFT 14 since it has no data during the mission
- Removed microSWIFT 4 since it has no data during the mission
- Removed microSWIFT 3 since it has no data during the mission
- Removed microSWIFT 17 since it has no data during the mission
- Removed microSWIFT 57 since it has no data during the mission
- Removed microSWIFT 60 since it has less than 500 data points during the mission
- Removed microSWIFT 23 since it has less than 500 data points during the mission
- Removed microSWIFT 12 since it has less than 500 data points during the mission
- Removed microSWIFT 56 since it has less than 500 data points during the mission
- Masked microSWIFT 37 from index 3000 to 6500 since it was being carried back out on surfboards and redeployed during this time
- Masked microSWIFT 18 from the start to index 5500 since it was not recording IMU measurements at this time, then from 7500 to 9000 since the IMU stopped recording during this interval again and then finally from index 14000 to the end since it had stopped IMU recording again.

Mission 36(Cleaned on 02/23/22):

- Adjusted start time from 2021-10-14T14:00:00 to 2021-10-14T14:20:00 since all of the microSWIFTs were not deployed at this point
- Adjusted end time from 2021-10-14T15:00:00 to 2021-10-14T14:37:00 since all of the microSWIFTs had reached the beach at this point as seen by removal of points passing the spatial threshold
- Masked microSWIFT 43 from index 3000 to the end since it reached the beach and rolled back down into the water afterwards.
- Removed microSWIFT 58 since it had a bad gyroscope measurement seen by completely flat lines
- Masked microSWIFT 33 from the start to index 500 since it had very small signals at this point suggesting that it had not been deployed yet.

Mission 37(Cleaned on 02/23/22):

- Adjusted start time from 2021-10-14T15:09:00 to 2021-10-14T15:14:20 since the microSWIFTs were still on the jetski at this point as seen by intense clustering and fast movements
- Adjusted end time from 2021-10-14T15:14:30 to 2021-10-14T15:20:00 since almost all of the microSWIFTs had made it to the beach at this point as seen by the spatial threshold cutting off the remaining data points
- Removed microSWIFT 18 since it is missing GPS data during this mission
- Removed microSWIFT 13 since it has a bad IMU - all measurements don't fluctuate

- Masked microSWIFT 3 from the start to index 1200 since it was still on the jetski seen by the fast alongshore motion
- Masked microSWIFT 4 from the start to index 200 since it was still on the jetski seen by the fast alongshore motion
- Masked microSWIFT 14 from the start to index 1000 since it was still on the jetski seen by the fast alongshore motion
- Masked microSWIFT 17 from the start to index 1200 since it was still on the jetski seen by the fast alongshore motion
- Masked microSWIFT 27 from the start to index 1300 since it was still on the jetski seen by the fast alongshore motion
- Masked microSWIFT 56 from the start to index 500 since it was still on the jetski seen by the fast alongshore motion
- Masked microSWIFT 57 from the start to index 200 since it was still on the jetski seen by the fast alongshore motion
- Masked microSWIFT 60 from the start to index 500 since it was still on the jetski seen by the fast alongshore motion - also masked from index 3000 to the end since it moved back across the spatial threshold
- Masked microSWIFT 19 from the start to index 600 since it was still on the jetski seen by the fast alongshore motion
- Masked microSWIFT 2 from the start to index 1200 since it was still on the jetski seen by the fast alongshore motion

Mission 38(Cleaned on 02/24/22):

- Adjusted end time from 2021-10-14T17:50:00 to 2021-10-14T17:45:00 since almost all of the microSWIFTs had reached the beach at this point
- Removed microSWIFT 4 since it is missing GPS data
- Removed microSWIFT 3 since it is missing GPS data
- Removed microSWIFT 2 since it is missing GPS data
- Removed microSWIFT 27 since it is missing GPS data
- Removed microSWIFT 18 since it is missing GPS data
- Removed microSWIFT 56 since it is missing GPS data
- Removed microSWIFT 58 since it has a bad gyroscope
- Removed microSWIFT 36 since it looks like it accidentally stayed with the jetski the whole time
- Masked microSWIFT 46 from the start to index 1000 since the microSWIFT is still on the jetski seen by moving alongshore at a non drifting speed
- Masked microSWIFT 31 from the start to index 1000 since it is moving alongshore on the jetski then masked from index 10000 since it has a nonfluctuating signal indicating it is most likely on the beach but is not being masked correctly
- Masked microSWIFT 19 from index 7000 to the end since it looks like it is picked up by the jetski since it is moving offshore - this is seen in the location moving alongshore then remaining stationary and the low fluctuations in the imu signals
- Masked microSWIFT 44 from the start to index 1000 since the microSWIFT is still on the jetski seen by moving alongshore at a non drifting speed

- Masked microSWIFT 43 from the start to index 1000 since the microSWIFT is still on the jetski seen by moving alongshore at a non drifting speed

- Masked microSWIFT 34 from the start to index 1000 since the microSWIFT is still on the jetski seen by moving alongshore at a non drifting speed

- Masked microSWIFT 33 from the start to index 2000 since the microSWIFT is still on the jetski seen by moving alongshore at a non drifting speed

- Masked microSWIFT 23 from the start to index 1000 since the microSWIFT is still on the jetski seen by moving alongshore at a non drifting speed

Mission 39(Cleaned on 02/25/22):

- Adjusted start time from 2021-10-15T16:00:00 to 2021-10-15T16:12:30 since the microSWIFTs had not yet been deployed at this point as seen by the

- Adjusted end time from 2021-10-15T17:00:00 to 2021-10-15T16:27:00 since all of the microSWIFTs were being picked up by the people on surfboards at this point

- Masked microSWIFT 14 from index 8000 to the end since it had been picked up by the surfboards at this point as seen by the dampened acceleration signals

- Masked microSWIFT 23 from index 3000 to 8000 since the microSWIFT was not recording properly at this time as seen by non fluctuating accelerations during this period

- Masked microSWIFT 42 from index 4500 to 7500 since the microSWIFT passed the spatial threshold but there are a few point in this range that did not get masked properly

- Masked microSWIFT 57 from index 5500 to 7500 since the microSWIFT passed the spatial threshold but there are a few point in this range that did not get masked properly

- Masked microSWIFT 46 from index 10000 to the end since it passed the spatial threshold and then briefly passed back over it.

Mission 40(Cleaned on 03/01/22):

- Adjusted the start time from 2021-10-15T17:00:00 to 2021-10-15T17:14:00 since all of the microSWIFTs were still on the surfboards at this point in the process before being deployed

- Adjusted the end time from 2021-10-15T18:00:00 to 2021-10-15T17:50:00 so that we avoid the 10 minute data gap from minute 50 to the top of the hour

- Masked microSWIFT 14 from index 25000 to the end since it had been picked up by the surfboard at this point

- Masked microSWIFT 23 from index 17000 to the end since it had been picked up by the surfboard at this point

- Masked microSWIFT 57 from index 16000 to the end since it had been picked up by the surfboard at this point

- Masked microSWIFT 19 from index 20000 to the end since it had been picked up by the surfboard at this point

- Masked microSWIFT 31 from index 15000 to the end since it had been picked up by the surfboard at this point

- Masked microSWIFT 46 from index 15000 to the end since it had been picked up by the surfboard at this point

Mission 41(Cleaned on 02/25/22):

- Adjusted start time from 2021-10-17T12:15:00 to 2021-10-17T12:16:30 the microSWIFTs were still on the jetski seen by the intense clustering and fast movement over to the deployment location

- Adjusted the end time from 2021-10-17T13:00:00 to 2021-10-17T12:23:00 since all of the microSWIFTs had reached the beach at this point except for one that moved very far from the domain.

- Removed microSWIFT 58 since it is has a bad gyroscope

- Masked microSWIFT 33 from the start to index 800 since it was still on the jetski as seen by the dampened signal compared to the rest of the record and a spike in acceleration.

- Masked microSWIFT 50 from the start to index 800 since it was still on the jetski as seen by the dampened signal compared to the rest of the record and a spike in acceleration.

- Masked microSWIFT 34 from the start to index 800 since it was still on the jetski as seen by the dampened signal compared to the rest of the record and a spike in acceleration.

Mission 42(Cleaned on 02/25/22):

- Adjusted start time from 2021-10-17T13:00:00 to 2021-10-17T13:18:00 since the microSWIFTs we still on the pier and on the jetski up until this point for the first batch

- Adjusted end time from 2021-10-17T14:00:00 to 2021-10-17T13:41:00 since all of the microSWIFTs had made it to the beach or left the bathymetry domain
- Removed microSWIFT 2 since it is missing GPS data
- Removed microSWIFT 58 since it has a bad gyroscope
- Removed microSWIFT 19 since it was missing GPS data in the updated times of the mission
- Masked microSWIFT 23 from index 5000 to the end since it was still on the jetski being deployed before this point
- Masked microSWIFT 4 from index 5000 to the end since it was still on the jetski being deployed before this point
- Masked microSWIFT 17 from index 5000 to the end since it was still on the jetski being deployed before this point
- Masked microSWIFT 10 from index 5000 to the end since it was still on the jetski being deployed before this point
- Masked microSWIFT 27 from index 5000 to the end since it was still on the jetski being deployed before this point
- Masked microSWIFT 16 from index 5000 to the end since it was still on the jetski being deployed before this point
- Masked microSWIFT 29 from index 5000 to the end since it was still on the jetski being deployed before this point

- Masked microSWIFT 56 from index 5000 to the end since it was still on the jetski being deployed before this point
- Masked microSWIFT 60 from index 5000 to the end since it was still on the jetski being deployed before this point
- Masked microSWIFT 59 from index 5000 to the end since it was still on the jetski being deployed before this point
- Masked microSWIFT 3 from index 5000 to the end since it was still on the jetski being deployed before this point

Mission 43(Cleaned on 02/25/22):

- Removed microSWIFT 31 since it is missing GPS data
- Masked microSWIFT 14 from the start to index 28000 since it had all flat , non-fluctuating values up until that point
- Masked microSWIFT 23 from the start to index 3000 since it had all flat , non-fluctuating values up until that point
- Masked microSWIFT 3 from the start to index 1000 since it had all flat , non-fluctuating values up until that point
- Masked microSWIFT 2 from the start to index 500 since it had all flat , non-fluctuating values up until that point
- Masked microSWIFT 46 from the start to index 3000 since it had all flat , non-fluctuating values up until that point

Mission 44(Cleaned on 02/25/22):

- Adjusted the start time from 2021-10-18T13:09:00 to 2021-10-18T13:11:00 since some of the microSWIFTs were still on the pier at this point as seen by non fluctuating accelerations

- Adjusted the end time from 2021-10-18T15:50:00 to 2021-10-18T13:50:00 since the microSWIFTs started leaving the domain and started being picked up by the people on surfboards shortly after this time.

- Removed microSWIFT 10 since it had a lot of time where the IMU data stopped

- Masked microSWIFT 20 from the start to index 2000 since the IMU was not recording until this point as seen by completely flat signals until index 2000

Mission 45(Cleaned on 02/25/22):

- Adjusted the start time from 2021-10-18T17:15:00 to 2021-10-18T17:19:00 since the microSWIFTs had not been deployed yet as seen by flat/ dampened IMU signals and almost stationary GPS signals

- Adjusted the end time from 2021-10-18T18:30:00 to 2021-10-18T17:40:00 since most of the microSWIFTs made it to the beach and the rest started being picked up at this point

- Removed microSWIFT 8 since it had a bad gyroscope only z axis gyro was working

- Removed microSWIFT 56 since it has a bad gyroscope that shows a large swooping curve rather than fluctuations

- Removed microSWIFT 58 since it has a bad gyroscope that is missing all data

Mission 46(Cleaned on 02/25/22):

- Adjusted the start time from 2021-10-19T12:03:00 to 2021-10-19T12:08:00 since the microSWIFTs had not been deployed yet as seen by flat signals
- Removed microSWIFT 41 since it is missing all data during mission
- Removed microSWIFT 44 since it is missing all data during mission
- Removed microSWIFT 42 since it is missing all data during mission

Mission 47(Cleaned on 02/28/22):

- Removed this mission altogether since it had almost no data due to the microSWIFTs being deployed so close to shore.

Mission 48(Cleaned on 02/28/22):

- Removed microSWIFT 49 since it was missing all data during the mission
- Removed microSWIFT 50 since it was missing all data during the mission
- Removed microSWIFT 41 since it had <500 data points during the mission
- Removed microSWIFT 31 since it had <500 data points during the mission
- Removed microSWIFT 44 since it had <500 data points during the mission
- Removed microSWIFT 33 since it had <500 data points during the mission
- Removed microSWIFT 35 since it had <500 data points during the mission

Mission 49(Cleaned on 04/3/22):

- Removed microSWIFT 49 since it has almost no data points (<500 points)
- Removed microSWIFT 42 since it has almost no data points (<500 points)

- Removed microSWIFT 33 since it has almost no data points (<500 points)
- Removed microSWIFT 35 since it has almost no data points (<500 points)
- Mask microSWIFT 46 from the start to index 2000 and from index 5000 to the end since it is out of the water at this point as seen by a flat signal

Mission 50(Cleaned on 02/28/22):

- Removed microSWIFT 27 since it is missing all data during the mission
- Removed microSWIFT 58 since it had a bad gyroscope
- Masked microSWIFT 14 from index 7000 to the end since it was still on the jetski at this point as seen by fast moving irregular locations
- Masked microSWIFT 34 from index 7500 to the end since it moved back offshore and was far outside of the bathymetry domain
- Masked microSWIFT 56 from index 7000 to the end since it was still on the jetski at this point as seen by fast moving irregular locations
- Masked microSWIFT 57 from index 7000 to the end since it was still on the jetski at this point as seen by fast moving irregular locations
- Masked microSWIFT 17 from index 7000 to the end since it was still on the jetski at this point as seen by fast moving irregular locations
- Masked microSWIFT 16 from index 7000 to the end since it was still on the jetski at this point as seen by fast moving irregular locations
- Masked microSWIFT 20 from index 7000 to the end since it was still on the jetski at this point as seen by fast moving irregular locations

- Masked microSWIFT 2 from index 7000 to the end since it was still on the jetski at this point as seen by fast moving irregular locations

- Masked microSWIFT 4 from index 7000 to the end since it was still on the jetski at this point as seen by fast moving irregular locations

Mission 51(Cleaned on 04/5/22):

- Adjusted the start time from 2021-10-22T14:00:00 to 2021-10-22T14:10:00 since both microSWIFTs entered the water at this point as given by hand written notes from Emma

- The following are a translation of Emma Nuss' hand written notes and conversations from time to indices for masking:

  - microSWIFT 40:
  - in water - 14:10:13 (masked start-156)
  - out of water - 14:10:30
  - in water - 14:10:31 (masked 360:372)
  - out of water - 14:10:47
  - in water - 14:12:09 (masked from 564:1548)
  - out of water - 14:13:28
  - in water - 14:13:42 (masked from 2496:2664) - not in a breaker during this stretch
  - out of water - 14:14:05
  - in water - 14:15:05 (masked from 2940:3660) - breaker occurred in this section
  - out of water - 14:16:55
  - in water - 14:23:41 (masked from 4980:17052) - not in a breaker during this stretch
  - out of water - 14:25:40

  - in water - 14:31:06 (masked from 18480:22392)
  - out of water - 14:31:32
  - in water - 14:32:29 (masked from 23076:23388)
  - out of water - 14:33:01
  - in water - 14:36:38 (masked from 23772:26376)
  - out of water - 14:37:14
  - in water - 14:39:37 (masked from 26808:28524) - breaker at 14:39:38(index 28536), breaker at 14:40:55(index 29460)
  - out of water - 14:41:18
  - in water - 14:41:30 (masked from 29736:29880) - in breaker (time not noted)
  - out of water - 14:42:22 (masked from 30504:end)

Mission 52(Cleaned on 03/16/22):

- This dataset needs much more work and has been omitted from analysis for now. While this may prove to be useful down the line it is particularly hard to determine when the microSWIFTs were in and out of the water during this mission.

Mission 53(Cleaned on 03/08/22):

- Removed from the dataset since this was not a "real" deployment - we were testing to see the differences if we switched the accelerometer range from +-2g to +-4g

Mission 54(Cleaned on 02/28/22):

- Masked microSWIFT 14 from the start to index 2000 since it was still on the surfboard at this time before being deployed

- Masked microSWIFT 19 from index 11000 to the end since it has been picked up by the surfboard as seen by dampened signals and non natural speed

- Masked microSWIFT 21 from index 11000 to the end since it has been picked up by the surfboard as seen by dampened signals and non natural speed
- Masked microSWIFT 20 from index 11000 to the end since it has been picked up by the surfboard as seen by dampened signals and non natural speed
- Masked microSWIFT 18 from index 10000 to the end since it has been picked up by the surfboard as seen by dampened signals and non natural speed
- Masked microSWIFT 16 from index 10000 to the end since it has been picked up by the surfboard as seen by dampened signals and non natural speed
- Masked microSWIFT 23 from index 12000 to the end since it has been picked up by the surfboard as seen by dampened signals and non natural speed

Mission 55(Cleaned on 02/28/22):

- Many are missing data and is a tiny mission - Removed from the overall dataset since there was such a small amount of data

Mission 56(Cleaned on 02/28/22):

- Adjusted the start time from 2021-10-25T17:10:00 to 2021-10-25T17:17:00 since most of the microSWIFTs were still being paddled out and placed in their array formation
- Adjusted the end time from 2021-10-25T18:24:00 to 2021-10-25T17:50:00 since almost all the microSWIFTs made it to the beach in this amount of time
- Removed microSWIFT 4 since it is missing all IMU data during the mission

Mission 57(Cleaned on 03/08/22):

- tiny mission from the jetski since they were thrown so close to shore that they almost immediately washed up on the beach - removed from cleaned dataset since it had such a small amount of data

Mission 58(Cleaned on 02/28/22):

- Adjusted the start time from 2021-10-26T13:38:00 to 2021-10-26T13:41:00 since the microSWIFTs were all on the jetski up until this point

- Adjusted the end time from 2021-10-26T14:34:00 to 2021-10-26T13:50:00 so that we can avoid the 10 minute gap in data in the mission and there was not much data after the 10 minute gap

Mission 59(Cleaned on 02/28/22):

- Adjusted the end time from 2021-10-26T16:50:00 to 2021-10-26T16:48:00 since the microSWIFTs had started being picked up at this point as seen by a dampening of the acceleration signals and the fast backwards movement of the microSWIFTs

Mission 60(Cleaned on 02/28/22):

- Adjusted the start time from 2021-10-27T14:30:00 to 2021-10-27T14:34:00 since they were still traveling on the helicopter to the drop location at this point

- Removed microSWIFT 45 since it has a bad gyroscope

- Removed microSWIFT 58 since it has a bad gyroscope

Mission 61(Cleaned on 04/03/22):

- Adjusted the end time from 2021-10-27T15:20:00 to 2021-10-27T15:18:00 since all of the microSWIFTs had reached the beach at this point

- Adjusted the start time from 2021-10-27T15:16:00 to 2021-10-27T15:16:30 since most of the microSWIFTs were still on the jetski at this point

- Mask microSWIFT 37 from index 400 to the end since it is moving suspicious fast as seen by very sparse points in the location most likely due to being picked up by the jetski

Mission 62(Cleaned on 04/03/22):

- Adjusted end time from 2021-10-27T15:48:00 to 2021-10-27T15:35:00 since all of the microSWIFTs had made it to the beach at this time

- Removed microSWIFT 18 due to missing GPS data during mission.

- Masked microSWIFT 40 from the start to index 200 since it is moving suspiciously fast as seen by very sparse GPS points

- Masked microSWIFT 41 from index 1500 to the end since it moves back across the spatial threshold briefly at this point

- Removed microSWIFT 48 since it has almost no usable data (<500 points)

- Removed microSWIFT 3 since it has almost no usable data (<100 points)

- Removed microSWIFT 38 since it has almost no data points (<500 points) and it appears to be moving suspiciously fast during this period as seen by spare GPS points

- Masked microSWIFT 17 from the start to index 500 and from index 1200 to the end since it briefly passes back over the spatial threshold here

- Removed microSWIFT 21 since it has no data (<50 points).

- Removed microSWIFT 43 since it has almost no data points (<100 points)

- Masked microSWIFT 29 from the start to index 100 since it is most likely still on the pier as seen by flat acceleration signals then a large spike then a normal looking wave signal
- Masked microSWIFT 73 from the start to index 300 since it is most likely still on the pier as seen by flat acceleration signals then a large spike then a normal looking wave signal
- Masked microSWIFT 34 from index 300 to the end since it passes the spatial threshold at this point and all points after that it briefly passes back over the spatial threshold
- Masked microSWIFT 50 from the start to index 400 since it is most likely still on the pier as seen by flat acceleration signals then a large spike then a normal looking wave signal
- Masked microSWIFT 35 from index 600 to the end since it passes the spatial threshold at this point and all points after that it briefly passes back over the spatial threshold

Mission 63(Cleaned on 04/03/22):

- Removed microSWIFT 23 since it is missing GPS data during mission
- Removed microSWIFT 72 since it is missing GPS data during mission
- Removed microSWIFT 27 since it is missing GPS data during mission
- Removed microSWIFT 33 since it is missing GPS data during mission
- Removed microSWIFT 40 since it had <500 data points
- Removed microSWIFT 41 since it had <500 data points
- Removed microSWIFT 24 since it is missing IMU data during the mission

- Removed microSWIFT 37 since it had <500 data points
- Removed microSWIFT 38 since it had <500 data points
- Removed microSWIFT 36 since it had <500 data points
- Removed microSWIFT 17 since it had <500 data points
- Removed microSWIFT 21 since it had <500 data points
- Removed microSWIFT 30 since it has very suspicious GPS data (super sparse)
- Removed microSWIFT 10 since it has very suspicious GPS data (super sparse)
- Removed microSWIFT 43 since it has almost no data <200 points
- Removed microSWIFT 18 since it has almost no data <200 points
- Removed microSWIFT 45 since it has almost no data <200 points
- Removed microSWIFT 16 since it has no data at all
- Removed microSWIFT 60 since it has no data at all
- Masked microSWIFT 42 from index 1000 to the end since it passes back over the spatial threshold at this point

Mission 64(Cleaned on 02/28/22):

- Removed mission 64 since most of the microSWIFTs have almost no data and the ones that do have data seem to be very suspicious - not worthwhile to clean this mission

Mission 65(Cleaned on 02/28/22):

- Removed this mission from the cleaned dataset since it had almost no data since the microSWIFTs were deployed so close to the shore

Mission 66(Cleaned on 02/28/22):

- Removed microSWIFT 48 since it is missing GPS data and IMU data during the mission
- Masked microSWIFT 23 from index 2800 to the end since it passed the spatial threshold then moved back across at this point
- Masked microSWIFT 64 from the start to index 1100 since it was not recording until this point as seen by a completely straight line which indicates spurious interpolation
- Masked microSWIFT 10 from the start to index 500 since it had not yet been deployed from the pier
- Masked microSWIFT 61 from index 4000 to the end since the remaining measurements were completely flat indicating it was on the beach or stationary
- Masked microSWIFT 29 from the start to index 500 since it had not yet been deployed from the pier
- Masked microSWIFT 38 from the start to index 1200 since it was not recording until this point as seen by a completely straight line which indicates spurious interpolation
- Masked microSWIFT 30 from the start to index 500 since it had not yet been deployed from the pier
- Masked microSWIFT 3 from the start to index 200 since it had not been deployed yet and from index 2500 to the end since it reached the beach and then crossed back across the spatial mask threshold

- Masked microSWIFT 12 from index 3000 to the end since it passed the spatial threshold then moved back across at this point

Mission 67(Cleaned on 02/28/22):

- Adjusted the start time from 2021-10-28T14:27:00 to 2021-10-28T14:30:00 since the microSWIFTs were still being deployed at this point from the pier as seen by movement along the pier

- Adjusted the end time from 2021-10-28T14:50:00 to 2021-10-28T14:46:00 since all of the microSWIFTs made it to the beach by this time

- Removed microSWIFT 19 since it had a bad IMU

- Masked microSWIFT 30 from index 3500 to the end since it passed the spatial threshold then passed back over it

- Masked microSWIFT 60 from index 8100 to the end since it stopped recording properly at this point as seen by non fluctuating signals

- Masked microSWIFT 29 from index 10000 to the end which has a few values that did not get masked properly

- Masked microSWIFT 72 from index 4200 to the end since it stopped recording properly as seen by flat and non-fluctuating values due to weird interpolations

Mission 68(Cleaned on 02/28/22):

- Adjusted the start time from 2021-10-28T15:30:00 to 2021-10-28T15:34:00 since most to the microSWIFTs were not in the water until this point

- Adjusted the end time from 2021-10-28T16:20:00 to 2021-10-28T15:50:00 so that we do not have to have the 10 minute data gap and many of the microSWIFTs had already made it to the beach at this point
- Removed microSWIFT 58 since it had a bad gyroscope
- Masked microSWIFT 23 from index 10000 to the end since it was no longer recording as seen by completely flat signals
- Masked microSWIFT 57 from index 2000 to the end since it was no longer recording as seen by completely flat signals
- Masked microSWIFT 29 from index 4500 to the end since it was no longer recording as seen by completely flat signals

Mission 69(Cleaned on 01/28/22):

- Adjusted the start time from 2021-10-28T17:05:00 to 2021-10-28T17:07:00 since that is when most of the microSWIFTs actually enter the water as seen by flat IMU signals.
- Adjusted end time from 2021-10-28T17:30:00 to 2021-10-28T17:20:00 since all microSWIFTs have reached the beach by this point.
- Note that microSWIFT 58 has bad gyroscope data - may need to be removed
- Mask microSWIFT 59 from the start to index 1800 since it had not been deployed yet as seen by stationary, nonfluctuating signals.
- Mask microSWIFT 57 from index 6000 to end since it reached the beach then rolled back down slightly.

Mission 70(Cleaned on 01/28/22):

- Adjusted start time from 2021-10-28T17:40:00 to 2021-10-28T17:41:00 since most microSWIFTs had not been deployed yet as seen by flat IMU signals.
- Adjusted end time from 2021-10-28T17:50:00 to 2021-10-28T17:45:00 since all microSWIFTs had made it to the beach at this point.
- Removed microSWIFTs 23, 48 due to missing GPS data

Mission 71(Cleaned on 02/14/22):

- Adjusted start time from 2021-10-28T18:04:00 to 2021-10-28T18:05:00 since microSWIFTs 41, 24, 64, 16 and 61 were not in the water yet as seen by a large spike in accelerations followed by normal wave signals
- Adjusted end time from 2021-10-28T18:20:00 to 2021-10-28T18:18:00 since all microSWIFTs had reached the beach by this point
- Removed microSWIFT 58 since it has a bad gyro
- Removed microSWIFT 45 since it had bad z axis gyro measurements as seen by a completely flat line
- Removed microSWIFT 59 since it had almost no data during the deployment (500 points or 45 seconds)
- Note: microSWIFT 30 has a bad magnetometer

Mission 72(Cleaned on 02/14/22):

- Removed microSWIFT 48 since it is missing GPS data
- Masked microSWIFT 49 from index 7000 to the end since it reached the beach indicated by a stationary acceleration signal and it wasn't cut off by the spatial mask

- Removed microSWIFT 45 since it has a bad gyroscope
- Removed microSWIFT 58 since it has a bad gyroscope

Mission 73(Cleaned on 02/14/22):

- Adjusted start time from 2021-10-28T19:10:00 to 2021-10-28T19:11:00 since most microSWIFTs were not in the water yet as seen by a spike in acceleration signals
- Adjusted end time from 2021-10-28T19:30:00 to 2021-10-28T19:21:00 since all microSWIFTs have reached the beach at this point as shown by the spatial mask
- Removed microSWIFT 58 since it has a bad gyro
- Note microSWIFT 50 has a bad magnetometer

Mission 74(Cleaned on 02/14/22):

- Adjusted start time from 2021-10-29T12:12:00 to 2021-10-29T12:13:30 since most microSWIFTs were not in the water yet as seen by a spike in acceleration signals
- Adjusted end time from 2021-10-29T12:40:00 to 2021-10-29T12:23:00 since most microSWIFTs had made it to the beach by this point
- Removed microSWIFT 58 since it has a bad gyroscope
- Removed microSWIFT 50 since it has a bad gyroscope
- Mask microSWIFT 12 from index 3500 to the end since it had a few points that were not successfully cut off by the spatial mask most likely due to the microSWIFT rolling back down the beach briefly

- Mask microSWIFT 62 from index 4500 to the end since it had a few points that were not successfully cut off by the spatial mask most likely due to the microSWIFT rolling back down the beach briefly

Mission 75(Cleaned on 02/14/22):

- Adjusted start time from 2021-10-29T13:02:00 to 2021-10-29T13:03:00 since a few of the microSWIFTs had not yet been deployed as seen by large spikes in accelerations at the start of the record

- Adjusted end time from 2021-10-29T13:20:00 to 2021-10-29T13:09:00 since all the microSWIFTs had made it to the beach at this point

- Removed microSWIFT 48 since it is missing GPS data

- Removed microSWIFT 26 since it is missing GPS data

- Removed microSWIFT 58 since it has a bad gyroscope

Mission 76(Cleaned on 02/14/22):

- Adjusted start time from 2021-10-29T13:28:00 to 2021-10-29T13:29:00 since a few microSWIFTs were not quite in the water yet as seen by spikes in acceleration signals

- Adjusted end time from 2021-10-29T13:44:00 to 2021-10-29T13:37:00 since almost all microSWIFTs had made it to the beach at this point

- Masked microSWIFT 54 from start to index 2000 since a few points weren't correctly masked at this time

- Removed microSWIFT 18 since it has almost no data during this mission

- Masked microSWIFT 60 from index 2000 to the end since it had landed on the beach already
- Masked microSWIFT 35 from index 4000 to end since a few points were not cut off correctly from spatial mask
- Removed microSWIFT 50 since it has a bad gyroscope
- Removed microSWIFT 58 since it has a bad gyroscope
- Removed microSWIFT 48 since it is missing GPS data
- Removed microSWIFT 26 since it is missing GPS data

Mission 77(Cleaned on 02/15/22):

- Adjusted start time from 2021-10-29T14:02:00 to 2021-10-29T14:02:45 since a few of the microSWIFTs were not quite in the water as shown by a spike in acceleration data at the beginning of the record
- Adjusted end time from 2021-10-29T14:18:00 to 2021-10-29T14:08:15 since almost all the microSWIFTs made it to the beach by this point as seen by the spatial mask
- Removed microSWIFT 64 since it is missing GPS data
- Removed microSWIFT 58 since it has a bad gyroscope
- Removed microSWIFT 48 since it is missing GPS data
- Removed microSWIFT 26 since it is missing GPS data
- Note that microSWIFT 76 has a bad magnetometer

- Masked microSWIFT 72 from index 3500 to the end since a few points were not fully cut off by the spatial mask
- Masked microSWIFT 62 from index 2500 to the end since a few points were not fully masked from the spatial mask
- Masked microSWIFT 60 from index 3000 to the end since a few points were not fully masked from the spatial mask

Mission 78(Cleaned on 02/15/22):

- Adjusted start time from 2021-10-29T14:28:00 to 2021-10-29T14:28:50 since a few of the microSWIFTs had not gotten into the water yet as seen by spikes in acceleration at the beginning of the record
- Adjusted the end time from 2021-10-29T14:47:00 to 2021-10-29T14:39:00 since most of the microSWIFTs had made it to the beach at this point
- Masked microSWIFT 42 from index 7000 to the end since a few point were not masked most likely due to it rolling back down the beach
- Masked microSWIFT 24 from index 5500 to the end since a few point were not masked most likely due to it rolling back down the beach
- Removed microSWIFT 61 since it had a bad gyroscope as seen by spurious/ suspicious large sweeping curves
- Removed microSWIFT 43 since it had a bad z axis gyro scope as seen by a completely flat line
- Removed microSWIFT 76 since the IMU was not working properly

- Removed microSWIFT 18 since it is missing GPS data
- Removed microSWIFT 58 since it has a bad gyroscope
- Removed microSWIFT 48 since it is missing GPS data
- Removed microSWIFT 26 since it is missing GPS data

Mission 79(Cleaned on 02/15/22):

- Adjusted start time from 2021-10-29T15:03:00 to 2021-10-29T15:04:30 since most of the microSWIFTs were not in the water yet
- Adjusted end time from 2021-10-29T15:16:00 to 2021-10-29T15:11:30 since almost all of the microSWIFTs were on the beach at this point which we can see by the spatial mask cutting it off at this point
- Masked microSWIFT 18 from index 4000 to the end since some of the points were not fully cutoff by the spatial mask most likely due to the microSWIFT rolling back down the beach
- Masked microSWIFT 37 from index 4500 to the end since some of the points were not fully cutoff by the spatial mask most likely due to the microSWIFT rolling back down the beach
- Removed microSWIFT 43 since it had a bad z axis gyroscope measurement seen by a completely flat signal
- Removed microSWIFT 16 since it had a suspicious gyroscope measurement which had large sweeping curves that look very nonphysical
- Removed microSWIFT 58 since it has a bad gyroscope

- Removed microSWIFT 48 since it is missing GPS data
- Removed microSWIFT 26 since it is missing GPS data
- Note that microSWIFT 18 also had a bad magnetometer

Mission 80(Cleaned on 02/15/22):

- Adjusted the start time from 2021-10-29T15:24:00 to 2021-10-29T15:26:00 since most of the microSWIFTs were not in the water quite yet as seen by spikes in acceleration
- Adjusted the end time from 2021-10-29T15:40:00 to 2021-10-29T15:32:30 since most of the microSWIFTs had reached the beach at this point as seen by most of the data being cut off by the spatial mask at this point
- Removed microSWIFT 64 since it had almost no data 500 points total during this mission
- Removed microSWIFT 18 since it had suspicious sweeping gyroscope measurements that are not physical
- Removed microSWIFT 43 since it had a bad z axis gyroscope as seen by a completely flat signal
- Removed microSWIFT 54 since it had a bad gyroscope
- Removed microSWIFT 58 since it has a bad gyroscope
- Removed microSWIFT 48 since it is missing GPS data
- Removed microSWIFT 26 since it is missing GPS data
- Note that microSWIFT 41 has a bad magnetometer

- Masked microSWIFT 12 from index 2200 to the end since it did not fully cutoff all points from the spatial mask most likely due to the microSWIFT rolling back down the beach

- Masked microSWIFT 10 from index 4000 to the end since it did not fully cutoff all points from the spatial mask most likely due to the microSWIFT rolling back down the beach

- Masked microSWIFT 60 from index 2500 to the end since it did not fully cutoff all points from the spatial mask most likely due to the microSWIFT rolling back down the beach

- Masked microSWIFT 57 from index 4000 to the end since it did not fully cutoff all points from the spatial mask most likely due to the microSWIFT rolling back down the beach

Mission 81(Cleaned on 02/15/22):

- Adjusted the end time from 2021-10-29T16:25:00 to 2021-10-29T16:16:30 since almost all of the microSWIFTs were on the beach at this point as seen by the cutoffs from the spatial mask

- Removed microSWIFT 40 since it has suspicious sweeping gyroscope measurement

- Removed microSWIFT 72 since it is missing GPS data during the mission

- Removed microSWIFT 41 since it is missing GPS data during the mission

- Removed microSWIFT 43 since it had a bad z axis gyroscope

- Removed microSWIFT 58 since it has a bad gyroscope

- Removed microSWIFT 48 since it is missing GPS data
- Removed microSWIFT 26 since it is missing GPS data